4D printing of shape memory polylactic acid (PLA)
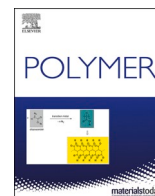
Mehrpouya, M.; Vahabi, H.; Janbaz, S.; Darafsheh, A.; Mazur, T.R.; Ramakrishna, S.

4D printing of shape memory polylactic acid (PLA)

Mehrshad Mehrpouya [a],*, Henri Vahabi [b], Shahram Janbaz [c], Arash Darafsheh [d], Thomas R. Mazur [d], Seeram Ramakrishna [e],**

[a] *Faculty of Engineering Technology, University of Twente, P.O. Box 217, 7500 AE, Enschede, the Netherlands*
[b] *Université de Lorraine, CentraleSupélec, LMOPS, F-57000, Metz, France*
[c] *Institute of Physics, Universiteit van Amsterdam, Science Park 904, 1098 XH, Amsterdam, the Netherlands*
[d] *Department of Radiation Oncology, Washington University School of Medicine, St. Louis, MO, 63110, USA*
[e] *Center for Nanofibers & Nanotechnology, National University of Singapore, Singapore*

ABSTRACT

Additive manufacturing has attracted much attention in the last decade as a principal growing sector of complex manufacturing. Precise layer-by-layer patterning of materials gives rise to novel designs and fabrication strategies that were previously not possible to realize with conventional techniques. Using suitable materials and organized variation in the printing settings, parts with time-dependent shapes that can be tuned through environmental stimuli can be realized. Given that these parts can either change their shape over time to a pre-programmed three-dimensional shape or revert to an initial design, this process has become referred to as four-dimensional (4D) printing. In this regard, the commonly-used polylactic acid (PLA) polymer has been recognized as a compelling material candidate for 4D printing as it is a biobased polymer with great shape memory behavior that can be employed in the design and manufacturing of a broad range of smart products. In this review, we investigate the material properties and shape memory behavior of PLA polymer in the first section. Then, we discuss the potential of PLA for 4D printing, including the principles underlying the strategy for PLA-based printing of self-folding structures. The resulting materials exhibit response to environmental stimulus as well as temperature, magnetic field, or light. We additionally discuss the impact of geometrical design and printing conditions on the functionality of the final printed products.

1. Introduction

The popularity of 3D printing has continuously increased since its origin in the early 1980s [1–4]. Since then, 3D printing has found diverse applications in manufacturing processes [5–7], product development and prototyping [8,9], and biotechnology [10,11]. In the meantime, novel applications have emerged rapidly in 3D printing techniques using advanced materials. Commonly-used 3D printing techniques in current practice include stereolithography (SLA), selective laser sintering/melting (SLS/SLM), laser engineering net shape (LENS), fused deposition modeling (FDM), material jetting (MJ), etc. [12–15]. Technologies for realizing these printing techniques have continued to become cheaper and more accessible.

An exciting recent development is 4D printing or precisely-controlled 3D printing in which materials can be deformed when exposed to an external stimulus [2,16–18]. Although 3D printing

techniques have been demonstrated for a multitude of materials including plastics, metals, and even ceramics, most materials cannot be applied to 4D printing because they do not exhibit sufficient shape change in the presence of stimuli such as humidity, temperature change, or an external magnetic field [2,19,20]. Candidate materials have to be printable and also exhibit "smartness", or the ability to be precisely manipulated by a stimulus [21,22]. Attempts continue to identify such smart materials to support the development of 4D printing technology [17,23–25].

Shape memory polymers (SMPs) have the ability to deform from an initial shape into a stress-free, temporally maintained shape until shape recovery is triggered by an external stimulus [26–28]. In particular, internal stress is built up during the programming process, and the stored energy can be released and provides the driving force in the shape recovery step. These shape changes are often achieved by varying temperature through a so-called transformation temperature. The
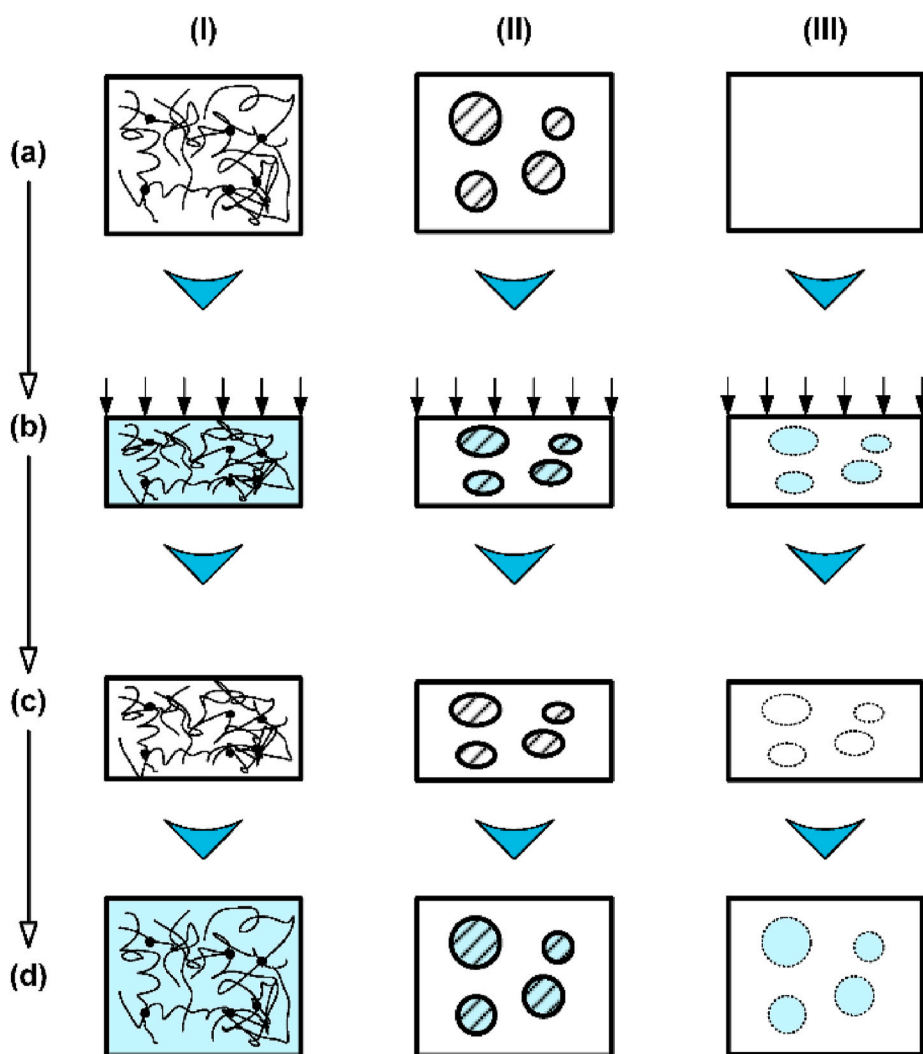

Fig. 1. Summary of mechanisms used for explaining shape memory behavior of heat-responsive polymers. (I) Dual-state mechanism (DSM) refers to materials that are relatively flexible and deformable above the T_g and hard upon cooling below this temperature (e.g., silicon) [45]; (II) Dual-component mechanism (DCM) corresponds to classes of materials with a soft and hard segmental structure in which each block can respond to temperature individually, e.g. polyurethane (PU) and olefin-block copolymers [46,47]; and (III) Partial-transition mechanism (PTM) refers to materials where heating may stop at a temperature within the transition range instead of complete transition taking place in the DSM and DCM in cases (I) and (II) [48]. In this figure: (a) shows the original sample at low temperatures, (b) is the sample upon heating and compressing, (c) is the sample after cooling and constraint removal, and (d) is the sample after heating for shape recovery [43]. (For interpretation of the references to colour in this figure legend, the reader is referred to the Web version of this article.)

part-specific process of transforming from a primary shape to an altered shape (and vice versa) in the presence of a stimulus is referred to as 'programming' [29–31]. SMPs, including those discussed in this review, are programmable and can achieve the desired shape transformation based on the printing techniques or the mechanical deformation of the fabricated product. Alternative materials include shape memory alloys (SMAs); however, SMPs have advantages such as lower cost, lower density, enabling greater recovery deformation, being biodegradable, and responding to more diverse stimuli [9,26]. SMPs have even shown potential for creating parts that automatically respond to environmental stimuli without the need for auxiliary actuation systems that demand additional power and hardware. There are currently two principal limitations of SMPs including low actuation stress and also long shape memory cycle time. Ongoing research is exploring associations between the composition and microstructure of SMPs to overcome these current limitations [32–35]. In this regard, polymer selection plays a key role in achieving programmable 4D printed structures.

From the polymer family, PLA has appeared as a compelling candidate for 4D printing thanks to its broad applications in 3D printing and low cost [36]. Although the shape-memory properties of PLA have been surveyed and reported, limited research exists on its application to shape deformation after 3D printing [37,38]. Much previously-published literature in this regard uses a blend of PLA with other polymers, like polyurethane (PU), to enhance shape recovery and to reduce the glass transition temperature (T_g) of PLA, thereby increasing its sensitivity to thermal programming [37,39]. The first section of this review

introduces PLA and its properties, particularly its shape memory behavior. Then, the second part investigates the application of PLA to 4D printing processes with emphasis placed on the impact of parameters – e. g., layer thickness, printing speed, nozzle, temperature, etc. – on 4D printing performance.

2. Polylactic acid (PLA)

2.1. Shape memory behavior

Several inherent properties are prerequisites for choosing any polymer to be programmed via printing. Viscoelasticity is the main characteristic of polymers giving them the ability to recover from a deformed state [40]. Polymer chains typically exhibit a specific response when exposed to an external force. Such an inherent response provides a polymer with a unique signature in terms of shape-memory behaviors. These signatures vary between families of polymers; however, tailoring the architecture of a polymer for a specific shape memory behavior continues to be an ongoing challenge. With current fabrication technologies, it has become possible to tailor polymer architectures for controlling shape memory properties [41,42]. In general, heat-responsive shape memory polymers can be described by one of three fundamental mechanisms, including the (I) dual-state (DSM), (II) dual-composite (DCM), and (III) partial-transition (PTM) mechanisms, as illustrated in Fig. 1 [36,43]. Silicone can be given as an example of the DSM. Since its T_g is below 0 °C, it is in a rubbery state at room
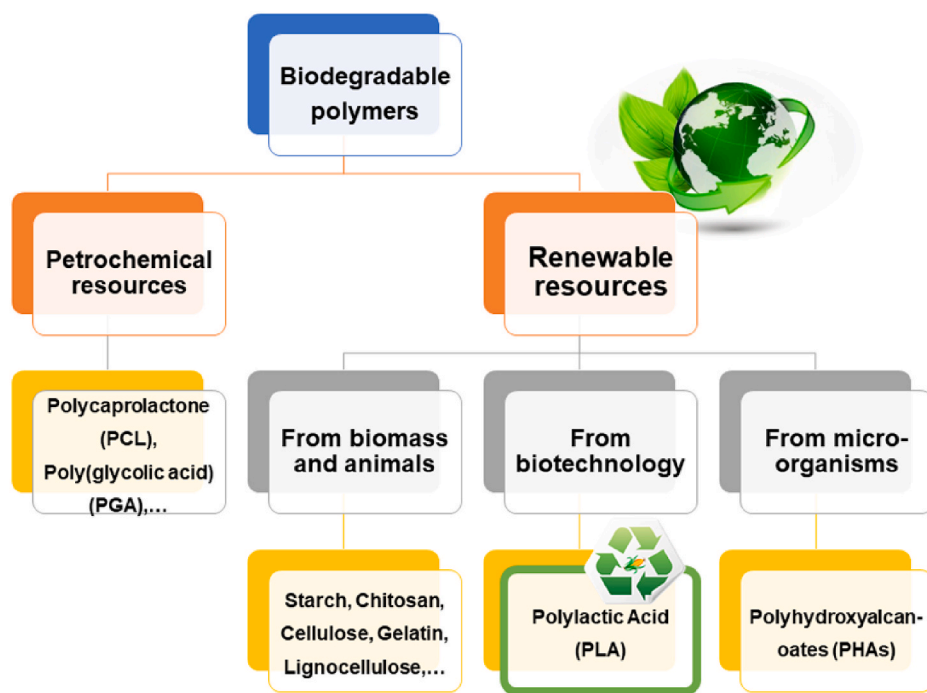
Fig. 2. Classification of poly(lactic acid) (PLA) relative to other biodegradable polymers. Biodegradable polymers are classified into two types according to their origins: petrochemical or renewable. Some biodegradable from petrochemical resources are polycaprolactone (PCL), poly(glycolic acid) (PGA), and poly(butylene succinate-co-adipate) (PBSA). Biodegradable polymers obtained from renewable resources are classified into three families: from biomass and animals (proteins and polysaccharides, e.g., starch, chitosan, cellulose, gelatin, lignocellulose), from biotechnology (PLA), and from microorganisms (e.g., poly(hydroxyalkanoates) (PHAs)).

temperature. If it is cooled and distorted below its T_g, it can maintain the distorted shape even if the distortion constraint is removed. Then, if it is heated to room temperature, it can reach its original shape. The DCM can be applied to ethylene-vinyl acetate (EVA) or PU which contain soft/hard segments. The shape memory effect can be achieved if at the temperature of interest the hard segment is elastic and the stiffness of the soft segment is significantly changed by heating, glass transition, or melting. A typical example ot PTM is poloxamer 407 (P407). If it is heated at a temperature within the transition range, the softened parts act as the transition component, and the un-softened part acts as the elastic component that stores elastic energy [44].

Designing a shape memory polymer requires fine-tuning the properties of materials. T_g and melting temperature (T_m) are two inherent properties that largely determine the shape memory response of
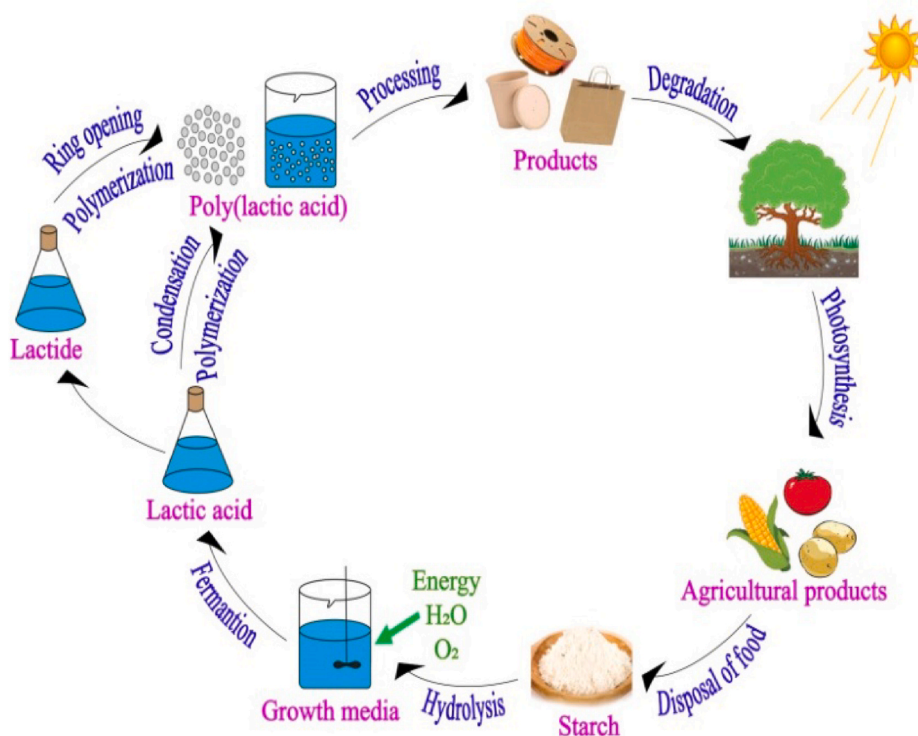

Fig. 3. The cycle of PLA, from synthesis to the end-of-life: 90 % of the total lactic acid produced in the world is currently obtained from bacterial fermentation of sugar. Two types of polymerization including ring-opening and condensation are usually used.
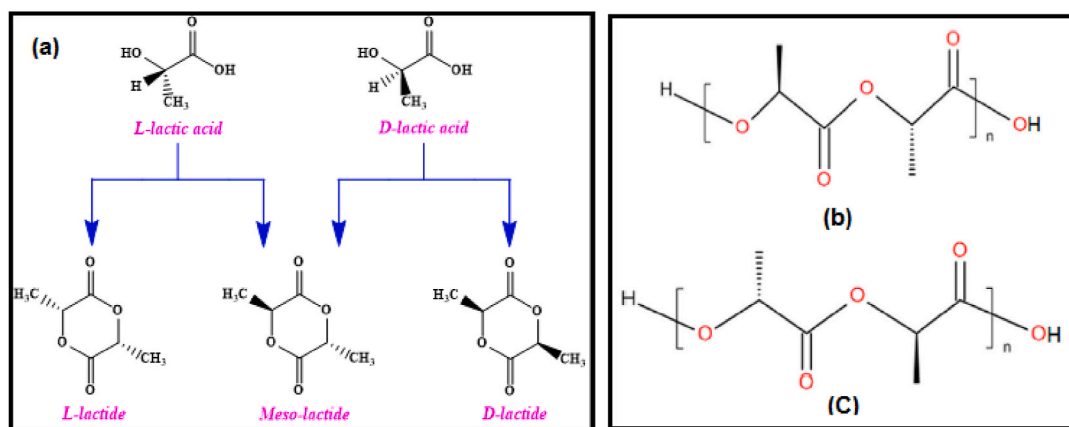
Fig. 4. Chemical structure of the stereoisomers of lactic acid (or 2-hydroxy propionic acid) and lactide (a), PLLA (b), and PDLA (c).

polymers [49]. The shape memory behavior of polymers is dependent on the presence of partially reversible covalent bonds and supra-molecular interactions [50]. By carefully and precisely crafting such properties, it is possible to enhance the shape memory behavior of polymer systems. For instance, by enhancing thermal conductivity the time to induction of shape recovery can be reduced. The elaborate material design may also yield shape memory polymers that respond to alternative impulses such as electricity, light, magnetism, and moisture [51].

Bio-based and biodegradable polymers have attracted significant attention in both academia and industry over the past decades [52–55]. Polylactic acid (PLA) is the most notable bio-sourced and biodegradable polymer in this family. PLA is best known as a biodegradable, biocompatible, and bio-based aliphatic polyester [56]. Fig. 2 displays the place of PLA between other biodegradable polymers. PLA was discovered in 1845 but commercialized in the early 1990s by the Cargill and the Dow Chemical Companies (TDCC) that launched the world's first PLA plant in Nebraska (Cargill Dow LLC) [57]. In 2005, Cargill bought out TDCC and the manufacturing company was re-named NatureWorks. Today, the principal producers of PLA in the world include NatureWorks (Ingeo), Total Corbion (Luminy), Synbra (BioFoam), Futero, Danimer Scientific LLC, Hisun, and Weforyou. The total annual production of PLA is currently estimated to be 200 kton/year. The global market for PLA was estimated to be USD 2.23 billion in 2017 and it is expected to grow by a stable compound annual growth rate (CAGR) of greater than 20.5 % from 2018 to 2026. Although packaging is the main application for PLA

in terms of volume, a report published in 2019 forecasted that the global market for PLA in 3D printing will expand at a CAGR of 19.3 % from 2018 to 2028 [58,59].

2.2. PLA properties

PLA is derived from lactic acid, or 2-hydroxy propionic acid, by bacterial fermentation from renewable resources such as corn, potato, cassava, and rice, as outlined in Fig. 3. Due to the presence of a chiral carbon, lactic acid has two enantiomers denoted as D- and L-lactic acid as shown in Fig. 4. From these enantiomers, lactide can be obtained via a two-step synthesis including oligomerization of lactic acid followed by cyclization [60]. Accordingly, three stereoisomers of lactide can be obtained, including L-lactide, D-lactide, and meso-lactide, as illustrated in Fig. 4.

Thus, three different grades of PLA can be synthesized including poly (D-lactic acid) (PDLA), poly(L-lactic acid) (PLLA), and a racemic polymer containing a random sequence of body enantiomers called poly(D, L-lactic acid) (PDLLA). Some properties of PLA are directly affected by variation in its stereochemistry. For example, there is no chain regularity for PDLLA and therefore it cannot be crystallized, while PLLA and PDLA are semi-crystalline PLAs. The melting point of PLA can be modulated by blending PLLA and PDLA. The variation of the melting point in this stereocomplex-PLA is 50 °C higher than that of PLLA and PDLA [61]. Since melting behavior has a significant effect on the
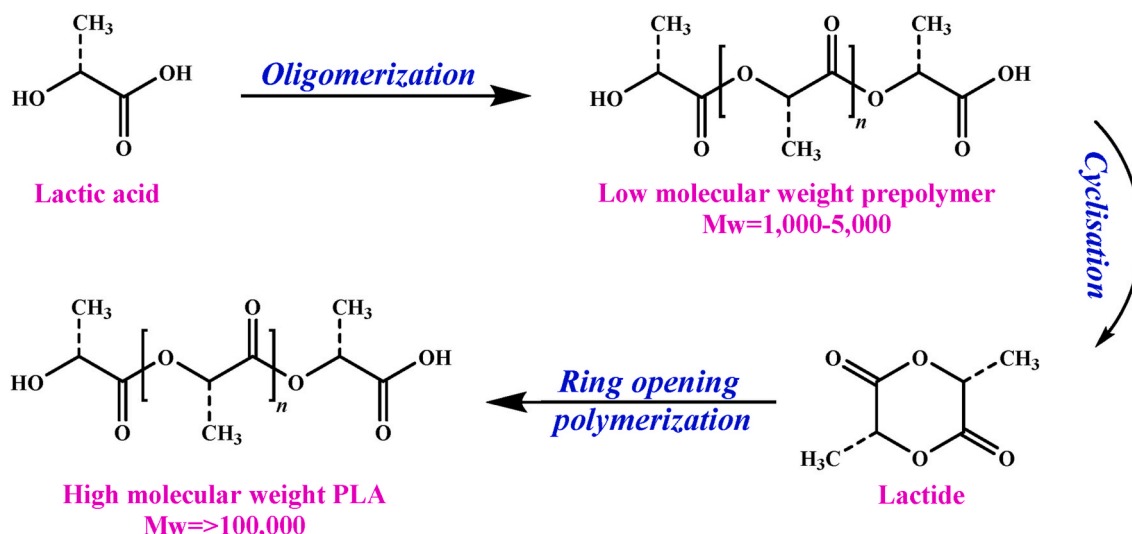

Fig. 5. Ring-Opening Polymerization (ROP) of lactide to produce PLA.

Table 1

Properties of three well-known commercially available PLA variants manufactured by Ingeo™ for 3D printing [65].

Properties	3D450[a]	3D850	3D870
Specific Gravity (g/cm^3)	1.32	1.24	1.22
MFR, g/10 min (210 °C, 2.16 kg)	18–26	7–9	9–15
Peak Melt Temperature (°C)	165	165–180	165–180
Glass Transition Temperature (°C)	55–60	55–60	55–60
Tensile Strength (MPa)	NA	50	40
Tensile Elongation, %	NA	3.31	NA
Tensile Modulus (MPa)	NA	2315	2685
3D Printing Temperature (°C)	NA	190–230	190–230

[a] *Commercialized in 2019.*

Table 2

The average values of glass transition temperature (T_g) and melt temperature (T_m) for various PLA copolymers [67].

Copolymer ratio	T_g (°C)	T_m (°C)
100/0 (L/D,L)	63	178
95/5 (L/D,L)	59	164
90/10 (L/D,L)	56	150
85/15 (L/D,L)	56	150
80/20 (L/D,L)	56	125

printability of polymers, a wide range of 4D printed products would be expected by using different families of PLA.

Specific applications for PLA in 3D and 4D printing depend on its underlying molecular structure, which in turn depends on the methods employed for PLA synthesis. Two main techniques are used for synthesizing PLA including polycondensation of lactic acid and ring-opening polymerization (ROP) of lactide [62,63]. Polycondensation is a simple approach, but the resulting PLA has a relatively low molecular weight (approximately 20,000 g/mol), the polymerization time is burdensomely long (typically more than 30 h), and water formed as a by-product must be eliminated to avoid further molecular weight reduction [64]. The second method, ROP, is the most-used technique consisting of the formation of lactide from lactic acid followed by ring-opening polymerization of lactide for obtaining high-molecular-weight PLA [62], as outlined in Fig. 5.

PLA variants used in 3D printing applications are generally produced via the ROP technique, and consequently should be more precisely referred to as "polylactide" rather than "poly(lactic acid)". Examples of commercial PLA options for 3D printing include three grades fabricated by NatureWorks, including variants 3D450, 3D850, and 3D870 having physical properties summarized in Table 1 [65].

For printing PLA, one needs to have a close look at its properties. PLA is a thermoplastic polymer that exhibits nearly 90 % light transmission comparable to that of glass. Its density is between 1.19 and 1.43 g/cm^{-3} depending on the exact manufacturing process. Its elastic modulus ranges between 2000 and 3500 MPa [66]. Its onset temperature of degradation (T_{onset}) is between 240 and 260 °C, which is sufficiently high to support its application in shaping processes. Values for these physical properties are representative of averages; precise values are sensitive to the relative content of D-lactide co-monomer within the polymer, which can depend on the manufacturing process. Table 2 summarizes variation in T_g and T_m for PLA consisting of varying ratios of co-monomers [67].

The molecular weight of PLA also significantly governs its T_g. It was recognized that the value of Tg for PLA has been shown to increase with increasing molecular weight up to a saturating weight between 80,000 and 100,000 g/mol, as illustrated in Fig. 6.

Above a threshold concentration of D-lactide co-monomer, PLA loses its ability to crystallize. More specifically, at 10 % mole percent concentration of D-lactide, PLA becomes amorphous. Moreover, different tacticities for PLA exhibit different T_g and T_m, as summarized in Table 3. Thermal properties of PLA are thus considerably affected by the synthesis procedure and post-crystallization process. While these variations may seem to be a hindrance to reliable fabrication, the manufacturing and processing dependence of PLA's characteristics introduce opportunities for tailoring properties for shape memory applications. For instance, prior literature has shown that PLA properties can be tuned through the addition of micro- and nano-particles or blending PLA with other polymers [69,70].

Most published research on shape memory properties of PLA investigate blends of PLA with other polymers such as PU and poly(ε-caprolactone) (PCL). These blends improve the shape recovery ratios (defined as the ability to recover the permanent shape) by decreasing the T_g of the resulting PLA. The most important parameter relating to the shape memory properties of PLA is its T_g. Below T_g, PLA possesses a permanent shape due to its ordered crystalline structure. Above T_g, PLA assumes a temporary shape because of intensified chain mobility. The melting temperature of PLA can also be considered as a transition temperature for shape memory applications. Given that T_m for PLA is approximately

Table 3

Values of T_g and T_m for PLAs having various tacticity.

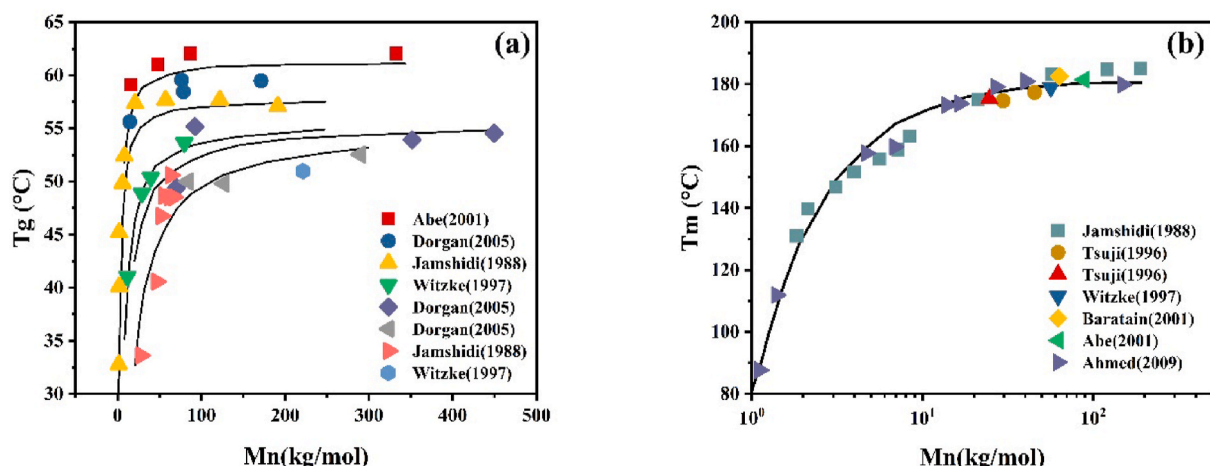| Tacticity	T_g (°C)	T_m (°C)
Isotactic	60	170
Syndiotactic	45	153
Atactic	55	amorphous

Fig. 6. Variation of T_g (a) and T_m (b) of PLA in different reports as a function of its molecular weight [68].
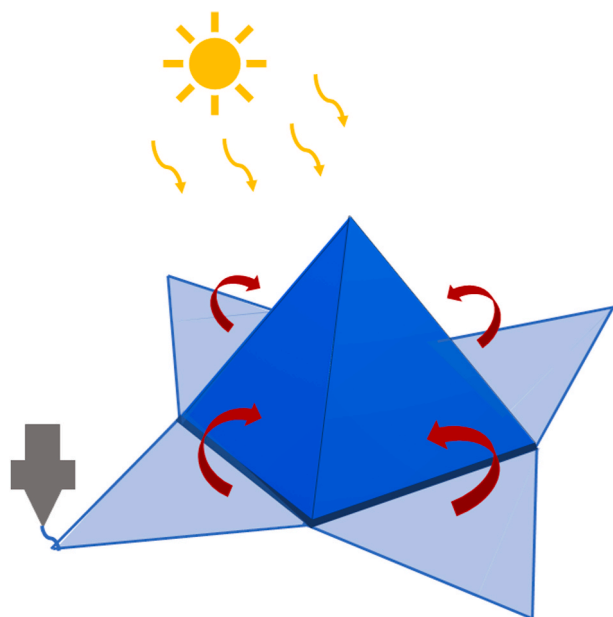
Fig. 7. Schematic overview of the 4D printing process of an origami pyramid; First, a conventional 3D printer fabricates a flat (origami) structure using SMP. Then an exposure to an external stimulus (like light or temperature) activates the smart materials and modifies the shape or function (in this case a pyramid shape).

160 °C, shape-memory applications near this transition exclude most biological applications where lower temperatures are required. Another challenge in exploiting T_m as an activating temperature is that PLA is typically in a semi-crystalline state including amorphous regions below this transition [43,71,72]. Generally, there are two domains in shape memory polymers: shape-fixing and shape-switching parts. The shape-fixing parts or net points are responsible for maintaining dimensional stability during distortion and recovery. The shape-switching parts consist of the long polymeric chains which store elastic energy. It is worth mentioning that the crystallization of long PLA chains can act as the net points [73–75].

Besides the synthesis variation described above, there are several alternative methodologies suggested in the literature for improving the programming behavior of PLA such as blending with other polymers, chemical or physical modification of PLA, and addition of nanofillers during the polymerization of PLA [76–78]. Different blends can improve the properties of PLA, specifically including non-biodegradable polymers that can improve the mechanical and thermal disadvantages of PLA. Candidate non-biodegradable polymers for blending with PLA include polyolefins [79–82], vinyl polymers [83,84], elastomers (e.g., polyolefin elastomer) [85] and rubbers (e.g., acrylonitrile–butadiene rubber, isoprene rubber) [86,87]. Biodegradable polymers that have been proposed for blending with PLA include polyanhydrides [88,89], aliphatic polyesters [90,91], aliphatic-aromatic copolyesters [92,93], elastomers, and rubbers [94]. The addition of nanofillers such as nanoclays, carbon nanotubes, nanocellulose, and inorganic nanoparticles [95–97] can also support overcoming the intrinsic drawbacks of PLA. For example, Cellulose nanocrystals (CNC) and silver (Ag) nanoparticles have improved gas barrier properties and antimicrobial activity in PLA-based films [98,99]. Nanoclays and carbon nanotubes have also been shown to improve thermal [100] and mechanical properties [101,102]. The shape of the nanofillers can affect the properties of the PLA-based polymer composites.
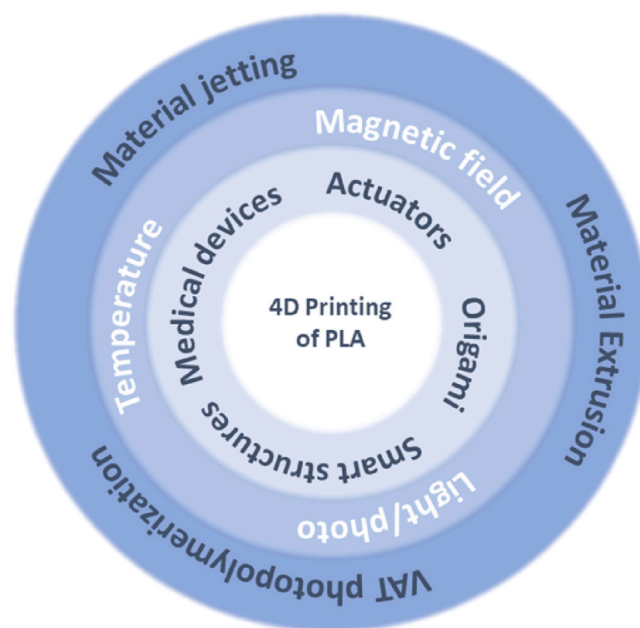

Fig. 8. 4D printing of PLA material enables the fabricated objects to change the shape or functionality after the printing process using various internal or external stimuli. This figure categorizes the 4D printing of PLA material into; 1) Printing techniques: Material extrusion, Material Jetting, Vat photopolymerization. 2) The stimulus for activation: thermal, magnetic field, and optical. 3) The application domains: medical devices, actuators, origami, and smart structures.

3. 4D printing of PLA

3.1. What is 4D printing?

4D printing was initially defined as 3D printing with the ability to alter a structural property or functionality over time [21,103–105]. To modify a 3D-printed structure and function after printing, materials must have unique characteristics that make them responsive to external stimuli. Such responsiveness can enable printed devices to be activated with specialized functions after the fabrication process. As 3D printing has been applied to SMPs, these materials can now be fabricated in complicated 2D and 3D shapes, as exemplified in Fig. 7, supporting novel transformations – and associated applications – upon being exposed to external impulses. 3D printers with multiple extruders support even more unique applications by fabricating parts that interlace SMPs with other materials.

4D printing in principle supports greater design freedom and can be applied to novel applications using adaptive materials, and improves capabilities of the printed products. By using conventional 3D printing techniques and selecting a material that responds accordingly to an environmental parameter such as moisture, temperature, pressure, or magnetic field, supplementary hardware is not required [106–108]. For example, SMPs can be programmed after printing to be flat to support packing and transportation, and then reverted to their intended functional shape. Such characteristics have engendered research interest for applications such as soft robotics, photovoltaic solar cells, deployable aerospace structures, and printable actuators for use in medical devices, textiles, defense, and aerospace [109].

3.2. 4D printing of PLA

Developing a new smart material for 4D printing is likely a time-intensive endeavor that requires iterative testing. Even if a material of suitable properties is identified and synthesized, the material must be able to be converted into a form that can be printed (e.g. PLA filament in
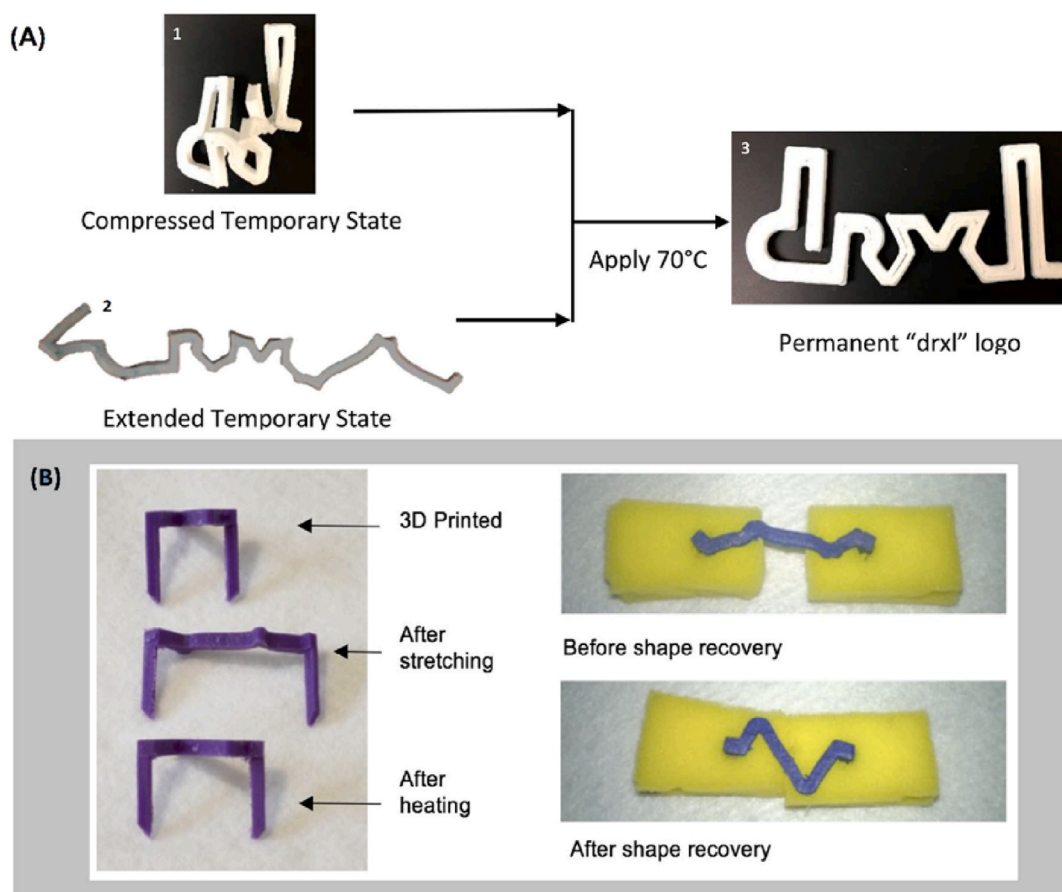
Fig. 9. (A) The programming process of a 3D printed 'drxl' logo fabricated by an FDM 3D printer; (1) first it is compressed, or (2) expanded after it has been heated above its T_g (70 °C), adjusted in shape, and then cooled, with (3) both shapes reverting to the initial shape when reheated to 70 °C in the absence of an applied force, reproduced from Ref. [122]; (B) Monolithic 3D printed staple, fabricated by FDM printer, with a tightening function enabled through heating and deformation, reproduced from Ref. [9].

the case of FDM printing). Such material must possess the capability of being configured into a well-defined shape when exposed to an external stimulus. Common stimuli in 4D printing applications are heat and water, with shape changes often transitioning between flat shapes and 3D objects.

PLA is a compelling material for FDM-3D printing due to its desirable properties including low T_g and shape memory [44,110–112]. Given that PLA is a well-established material for 3D printing, its application to 4D printing depends mostly on part design rather than any basic science associated with developing novel materials. PLA presents other advantages, including biocompatibility, biological inertness, and biodegradability, that suggest its applications to the biomedical field as well [113–117]. Fig. 8 highlights classes of the fabrication methods, stimuli, and applications for 4D printing of PLA material. The fabrication methods are categorized into the groups of material extrusion (e. g. fused deposition modeling-FDM/fused filament fabrication-FFF), material jetting (e. g. Inkjet), and vat photopolymerization (e. g. liquid crystal display-LCD). Applications span the micro-to macro-scale and include diverse areas of interest such as medical devices, smart actuators, and structures for prototyping.

PLA retains a permanent shape in a glassy state below T_g; however, once above T_g, PLA becomes sufficiently pliable to achieve deformation into a transient, alternative form. This temporary shape can be set if the force supporting the deformation is maintained as the temperature is reduced below T_g. Likewise, the original, permanent state can be restored upon reheating above T_g and removing this force [118–120]. Hanon et al. reported that 3D printed products can have a high dimensional accuracy of up to 98.81 % that indicates the great

capability of PLA for commercial FDM 3D printing process as a high quality and inexpensive method for producing parts [121]. Fig. 9 (A) represents a very simple example of the programming process for a logo fabricated by an FDM printer: by heating above T_g the logo can be programmed into a compressed or extended state, and by subsequently re-heating the logo can be reverted to its initial form. Given its biocompatibility and biodegradability, an especially compelling 4D printing application of PLA is surgical staples [122,123]. Fig. 9 (B) shows the concept for a monolithic, PLA-based suture with a self-tightening mechanism. For any 4D printing applications, the magnitude of shape-change can be tuned through non-uniform material filling and by strategically designing the interior lattice specifically in terms of its density and morphology [9,106].

Internal strain and stress created during conventional FDM-based 3D printing have been exploited to induce pattern formation [17,39,104]. In FDM printing, a filament is extruded through a heated nozzle. Upon extrusion on a print bed or previously-deposited layer, PLA cools and solidifies. The environmental conditions have a direct impact on the PLA polymer during the manufacturing process. For example, the humidity has a considerable effect on the material properties such that PLA is stronger in a dry atmosphere but very rigid. Therefore, the sample can break more easily in a dryer environment [124–126]. In this process, internal stress and strain are created due to traction forces created by the motor feeding the filament, which typically poses an undesirable effect in 3D printing signified by the shrinkage of parts upon cooling. Fig. 10 (A-B) exemplifies the shrinkage of a regular lattice upon removal from a water bath at 70 °C [17,39]. Such stored strain and stress can be utilized to make active shape change without requiring programming via an
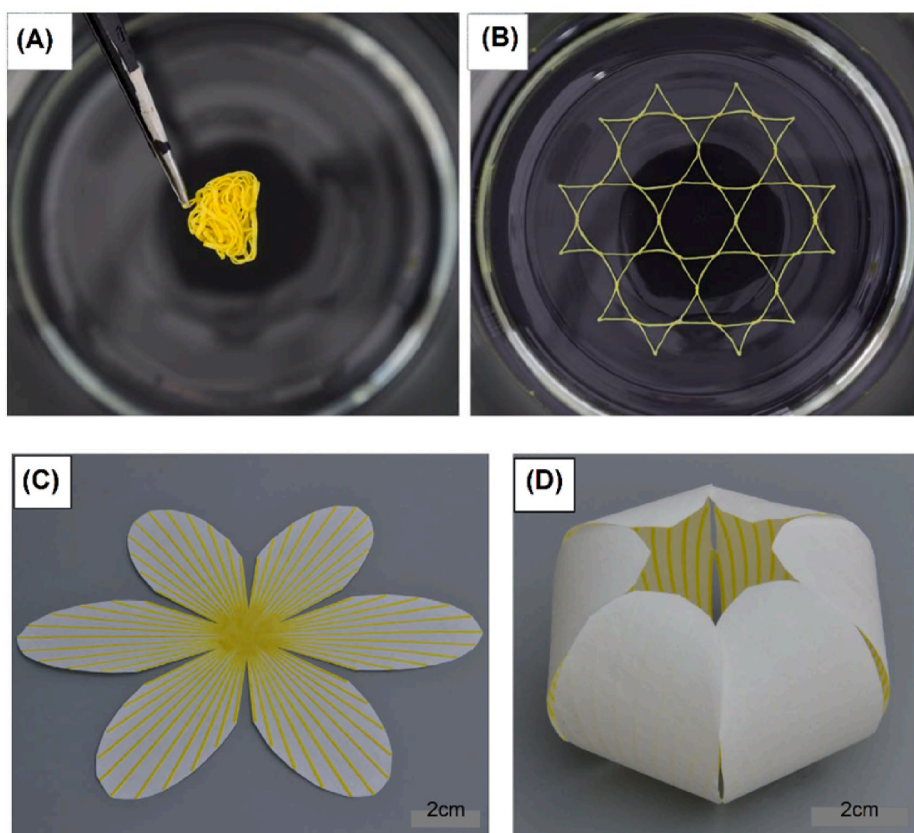
Fig. 10. Example of the strain-induced unfolding of a PLA-based component, manufactured by an FDM printer. (A) Irregular, the temporary shape of a folded two-dimensional (2D) lattice upon removal from 70 °C water, (B) Recovered, the initial shape of the 2D lattice when re-immersed in 70 °C water, exhibiting a shape memory effect, reproduced from Ref. [39]; (C) The initial shape of the sheet with strips oriented radially outward from a central point, (D) The final flower-like 3D shape achieved after heating and cooling the structure, reproduced from Ref. [127].
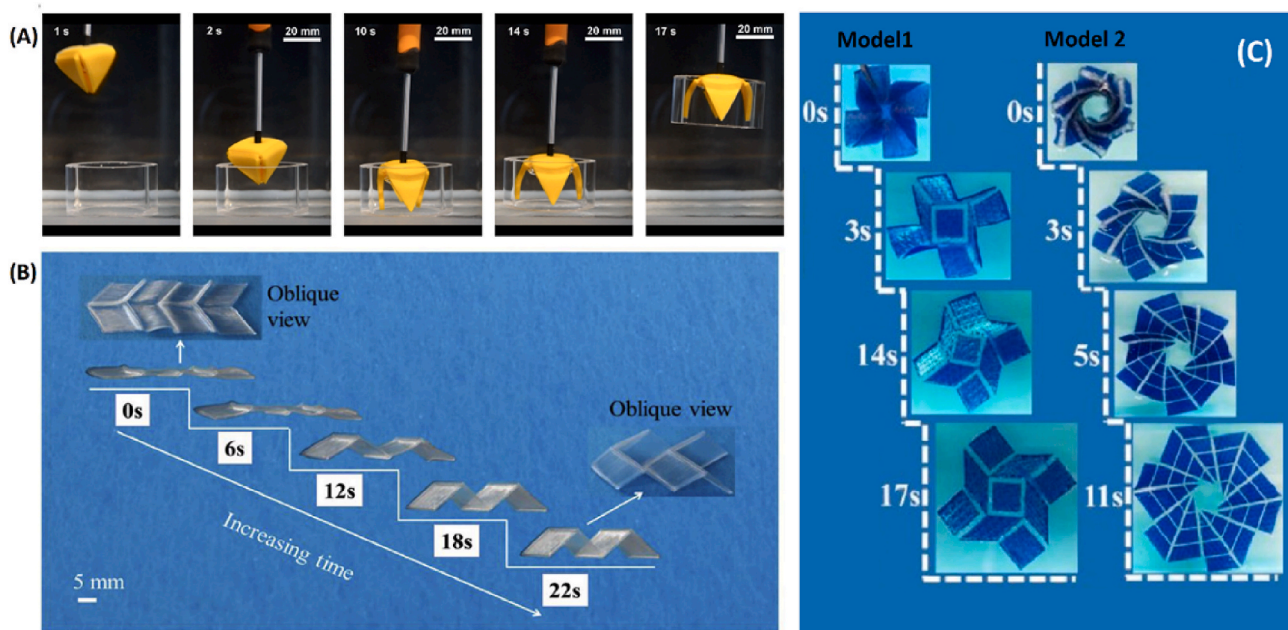
Fig. 11. The functionality and applications of the programmed origami structures, fabricated by FDM printer, (A) The application of 4D printed origami pyramid for grasping an object, reproduced from Ref. [129], (B) Shape recovery process of Miura-origami structure at 90 °C temperature, reproduced from Ref. [130], (C) Shape recovery process of two origami models from folded to flat state, reproduced from Ref. [131].

additional external force. By controlling strain in a 3D printed structure, the energy released upon heating the material above Tg can drive the desired change in shape. For example, Zhang et al. demonstrated that a 2D lattice could be controllably transformed into a flower-like 3D structure upon re-heating. As shown in Fig. 10 (C-D), PLA strips were printed via FFF-based 3D printing on a paper sheet in a series of petals oriented radially outward from a central point. Upon cutting the outline of the strips into the paper and heating the sheet with the PLA upward, the strips folded upward into a flower-like structure upon removing the heat and cooling to room temperature. When the structure was

Fig. 12. (A) The shape recovery process of the fabricated cylindrical shell using an LCD 3D printer, reproduced from Ref. [132]; (B) The schematic of the smart sandwich structure and the time-dep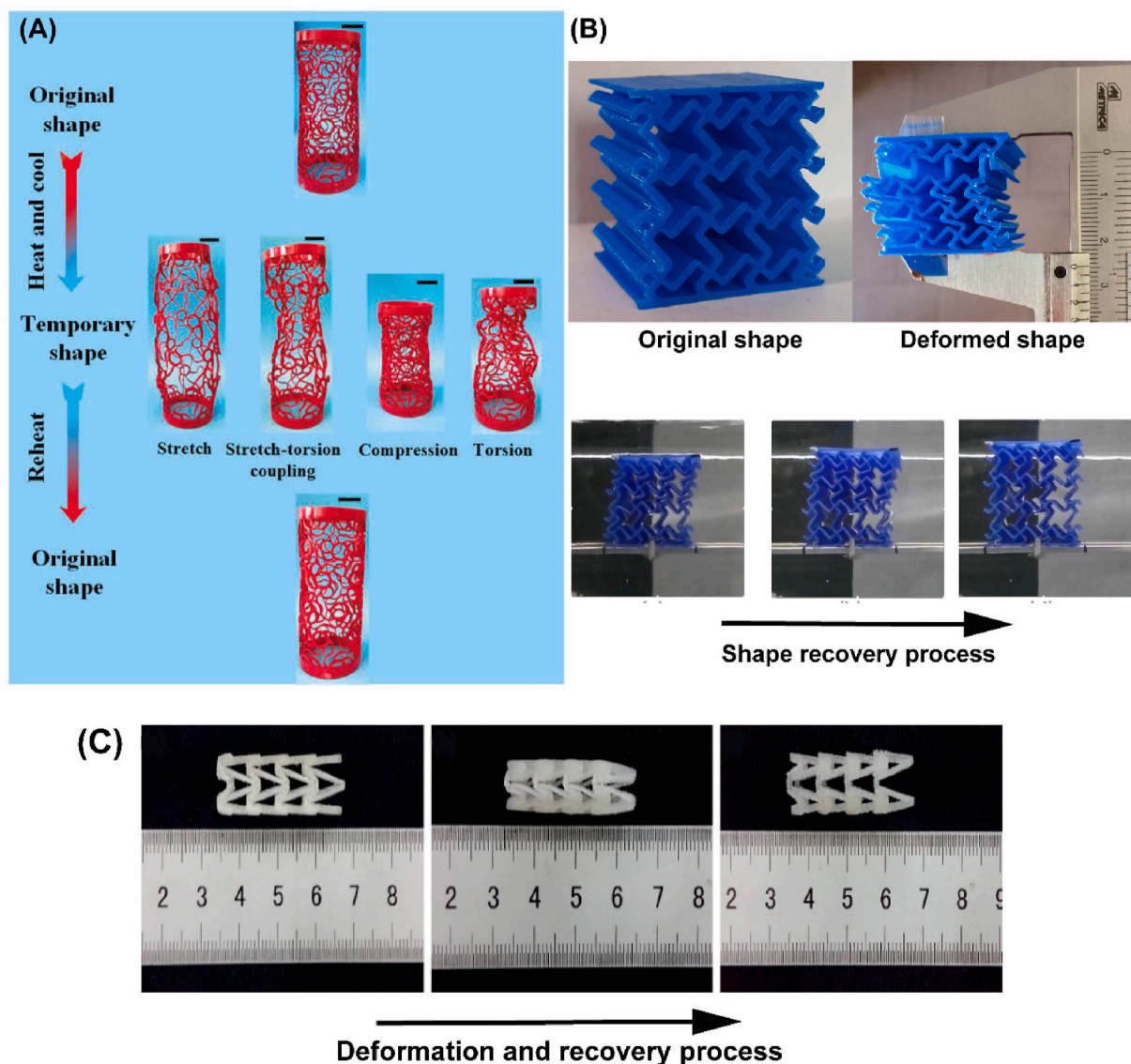endent recovery process of a deformed sample in a hot water bath, reproduced from Ref. [137]; (C) The deformation and shape recovery process of a PLA stent, reproduced from Ref. [141].

re-heated, the flower structure reverted its planar configuration [17, 127,128].

Mehrpouya et al. [129] also fabricated a foldable origami product using PLA filament and an FDM 3D printer. In particular, they programmed the printed structures using external mechanical forces so that they can be activated upon reaching the transition temperature and restored to their initial flat shape. This approach can be applied in the design and fabrication of various smart products. Fig. 11(A) shows the functionality of the programmed origami pyramid that can be used as a gripper for grasping an object. *Liu* et al. [130] also designed and fabricated a Miura-origami sheet using PLA with shape memory behavior. As shown in Fig. 11(B), the deformed tessellation specimen recovers the initial S-shape at the temperature of 90 °C in 22 seconds. In another study, *Xin* et al. designed and fabricated origami structures that could store strain and then release it via temperature stimulus. Fig. 11(C) illustrates the deployment process of the printed structures upon heating in hot water. The programmed structures recovered the initial flat shape in less than 20 seconds (depending on the design and geometry).

Xin et al. applied a photopolymerization 3D printer to fabricate chiral metamaterials with a photocurable polylactic acid (PLA)-based shape

memory polymer and using a light-curing 3D printer. The fabricated structures were programmable and tenable with the capability of bending in a large deformation with application to biomaterials as well as organs and tissues [132–136]. Fig. 12 (A) shows a cylindrical shell with auxetic behavior that can mimic blood vessels with similar mechanical properties and geometry. This figure exemplifies that the deformed structures, after stretching, twisting, and compressing, can perfectly recover their initial shape. *Barletta* et al. fabricated a complex geometry with potential as a stress-absorber using an FDM printer. Fig. 12 (B) illustrates the shape recovery process of the deformed sample in the hot water bath and the experimental results proved that the PLA component with various core designs has a proper shape memory effect so that it can retrieve the initial shape after any deformation quickly. Among different parameters, the activation temperature was found the most effective parameter with a high recovery time in a very short time [137–140]. *Wu* et al. also investigated the application of PLA material for the fabrication of self-expansion vascular stents using an FDM printer and a water-solvable support material. The PLA printed stent was capable of expanding in both longitudinal and radial directions below the glass temperature, and then it could recover the original cylindrical
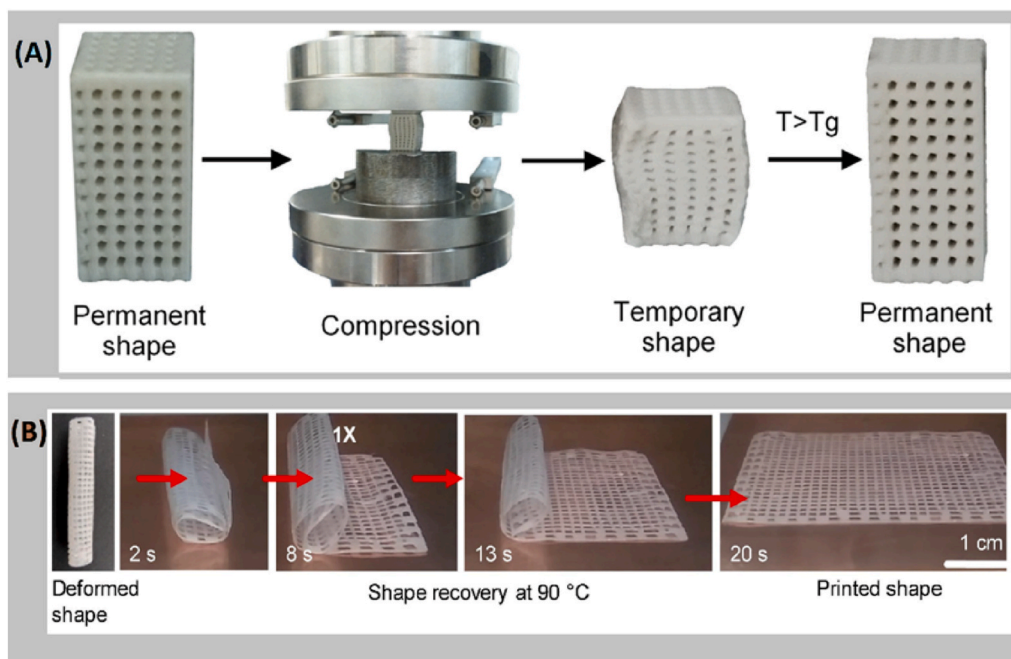
Fig. 13. (A) The recovery process of a 3D printed PLA/HA scaffold after the compression test and heating to above T_g, reproduced from Ref. [31]; (B) The shape recovery process of printed PLA/PEA structure at 90°, reproduced from Ref. [147].

shape up to 98 % above 65 °C. Fig. 12 (C) shows the initial printed sample, deformation and shape recovery process [141].

The combination of PLA with other polymers can provide an opportunity to enhance the functionality or add the other properties of the material. There are some studies on 4D printing of the modified PLA with various applications as well as biomedical and tissue engineering fields [17,142–146]. Novel 4D applications have been demonstrated combination of PLA with other polymers to enhance material functionality and properties. An exciting direction is tissue engineering via 3D printed parts that integrate a bioactive component with PLA. For example, *Senatov* et al. [31] fabricated combined PLA with hydroxyapatite (HA), a bioactive component that enhances osseointegration and improves the modulus of the composite. More specifically, the authors combined PLA with 15 % HA concentration as a candidate material for potentially repairing bone defects. Fig. 13 (A) shows a sample structure printed with this material combination via the FFF-based 3D printing process. Compression tests were performed on these structures to characterize shape recovery after heating above T_g. After a single compression cycle, parts exhibited a shape recovery of greater than 98 %. In comparison to PLA-only parts, the composite structures exhibited greater yield strength and Young's modulus and ultimately withstood larger numbers of compression cycles before being destroyed. These favorable characteristics suggest potential self-healing functionality that could be favorable in biomedical applications that require the prevention of crack propagation. Bodkhe and Ermanni [147] investigated a separate composite material for potential biomedical applications that can simultaneously achieve actuation and sensing. The investigated material combined PLA and polyesteramide (PEA) for shape-memory with added barium titanate (BT) nanoparticles to support piezoelectric sensing. The composite material was prepared as ink that was loaded into a syringe barrel for deposition via electric poling-assisted additive manufacturing (EPAM). Fig. 13 (B) shows a flat mesh fabricated with 96 wt% PLA plus 4 wt% PEA. After heating the mesh to 90° C in an oven and rolling it into a cylinder, a cylindrical shape could be fixed upon cooling to room temperature. When heated again to 90° C, the sheet reverted to its initial flat shape.

In an alternative composite that incorporated nanoparticles, *Wei* et al. [148] applied an inkjet 3D printer followed by UV curing in order to introduce Fe_3O_4 nanoparticles in PLA ink for enabling remote part heating via an externally applied, alternating magnetic field. Parts were printed through direct-write techniques using inks prepared from PLA with Fe_3O_4 nanoparticles introduced. As illustrated schematically in Fig. 14(A), ultraviolet light is applied in the printing process to induce a cross-linking reaction that supports shape-memory behavior. Through this process, the authors fabricated various complex shapes such as the stent tube with a diameter of 2.4 mm and 12.8 mm length as presented on the left side. As outlined in Fig. 14(B), nanoparticles in the PLA ink enable shape recovery through the application of a 30 kHz alternating magnetic field to induce heating that reverts a compressed cylinder into a cylinder with a circular cross-section [148,149]. In a separate example combining PLA with Fe_3O_4 nanoparticles, *Zhao* et al. [150] fabricated a tracheal scaffold by applying PLA/Fe_3O_4 filament via FDM printing. Similarly, by applying a 30 kHz alternating magnetic field, a flat scaffold can be induced to revert to its initial cylindrical shape within 35 s as shown in Fig. 14 (C). The motivation for this design is the possibility of implanting such a scaffold in the body in its temporary configuration and then applying an alternating magnetic field to restore a cylindrical shape that is adapted to fit the soft-tissue target within the body.

3.3. The effect of printing parameters

As 3D printing has grown in popularity, many 3D printer manufacturers have appeared with novel printing technologies and printable materials. Printers exist for many types of 3D printing with options suitable for both industrial and hobbyist applications. Different printers offer varying amounts of user control in the printing process through tunable parameters in software. Examples of such parameters include infill pattern, layer thickness, extruder nozzle temperature, extruder speed, build plate temperature, cooling fan speed, and several outline shells. Through iterative adjustment of these parameters, the quality of the print can be tailored according to the desired properties of a product [151]. For instance, increasing infill percentage can increase the effective density of a part, and reducing layer thickness can improve the quality of fine features on a design. While extensive literature has been published on the impact of parameter selection on print quality and mechanical properties, few studies exist on the impact of processing
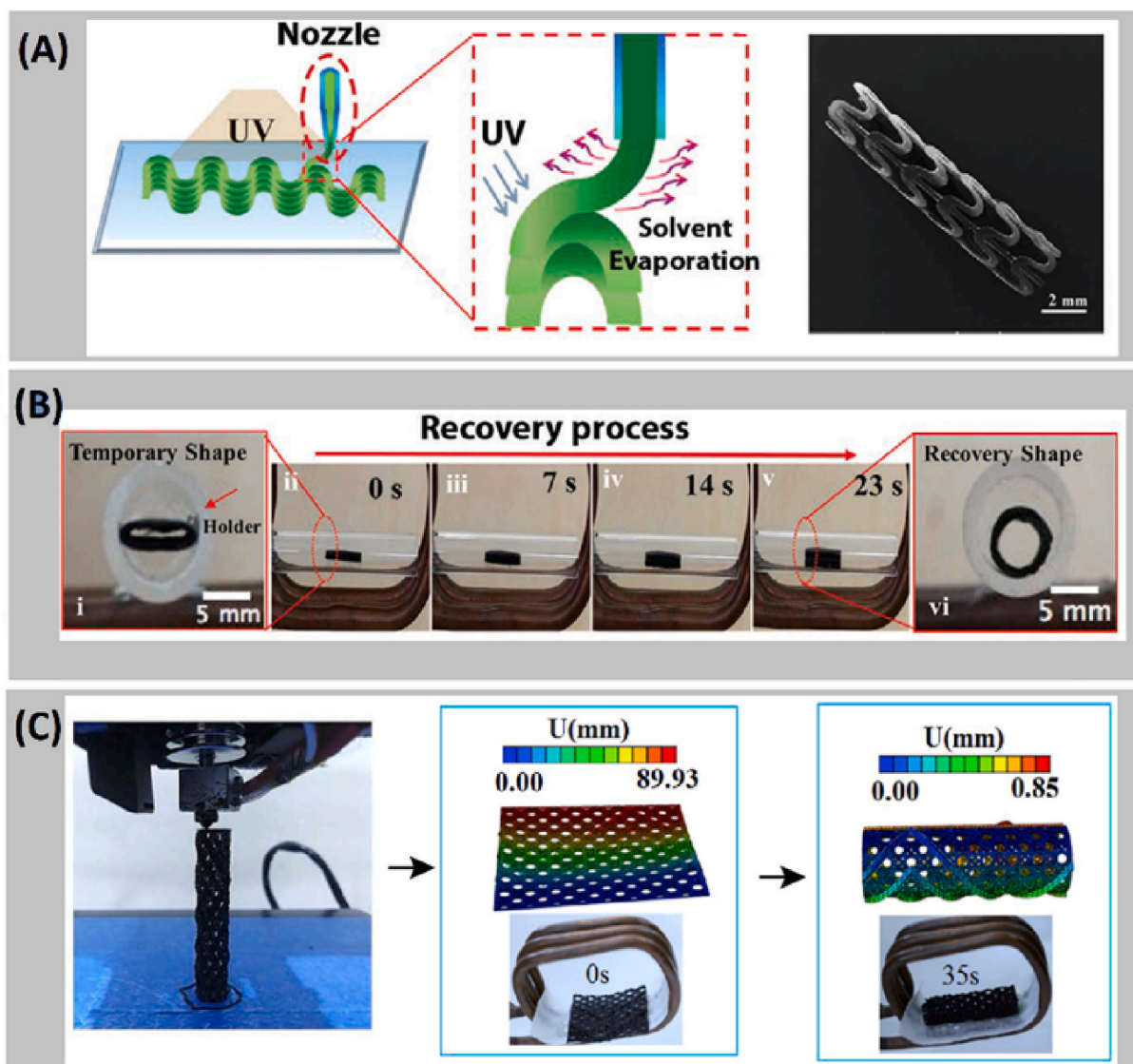
Fig. 14. (A) A schematic of printing process UV cross-linking PLA/Fe3O4 ink (left), SEM image of a 4D printed structure (right), reproduced from Ref. [148]; (B) Shape recovery process of 4D printed nanocomposite cylinder under a magnetic field, reproduced from Ref. [148]; (C) 3D printed PLA/Fe3O4 scaffold and the shape recovery process, reproduced from Ref. [150].

parameters on shape memory effects.

PLA filaments that are extruded in 3D printing decrease their length and thicken their diameter when heated above their T_g. The percentage decrease in length can in principle be tuned by varying printing parameters such as the extrusion and activation temperatures and the layer thickness [151,152]. *Van Manen* et al. [153] investigated the effect of printing patterns and parameters on the functionality of designed parts. Fig. 15(A) illustrates the concept of shape programming during the printing process so that the fabricated object can have self-bending or self-twisting based on pre-designed printing orientations (top). Also, strain in these layers depends strongly on basic printing parameters including nozzle temperature, layer thickness, and activation temperature as shown at the bottom. In another study, *Leist* et al. [122] printed PLA samples of varying thickness using an FDM 3D printer with in-plane dimensions of 10 mm width and 40 mm length. As shown in Fig. 15(B), samples with thicknesses of 800, 1000, and 1200 μm were prepared as cantilevers. Upon heat activation at 65 °C, cantilevers were nominally bent to a 90° angle and subsequently cooled to room temperature to achieve a programmed terminal angle α. Upon submersion in a heated water bath, the bent cantilever reverts to an unbent state with an

associated angle α′. As shown in Fig. 15(B), cantilevers exhibited large temperature- and thickness-dependent variation in this terminal angle α′. In general, increased cantilever thickness yielded a lower bending angle and slower bending rates. Both the bending angle and rate for each cantilever thickness increased in higher temperature baths [122,138, 154].

Wu et al. [155] tested variation in shape-recovery ratio R_r and the maximum shape-recovery rate V_m for 3D printed PLA for varying layer thickness H, raster angle Θ, deformation temperature T_d, and recovery temperature T_r. Fig. 15(C) shows the schematic of deformed and shape recovered samples on the top, and also the curves obtained for R_r as a function of time under identical deformation temperatures but varying recovery temperatures, raster angles, and layer thicknesses on the bottom [155]. Curves *a* and *b*– corresponding to the highest recovery temperatures – exhibit the most complete recovery at the fastest rate. These data highlight that among tested parameters, recovery temperature most significantly impacted the shape-recovery ratio for PLA. In the study, the T_g of PLA was measured to be approximately 63.5 °C according to dynamic mechanical analysis (DMA). For curves *a* and *b* where T_r exceeds this temperature, the PLA is heated into a rubbery state
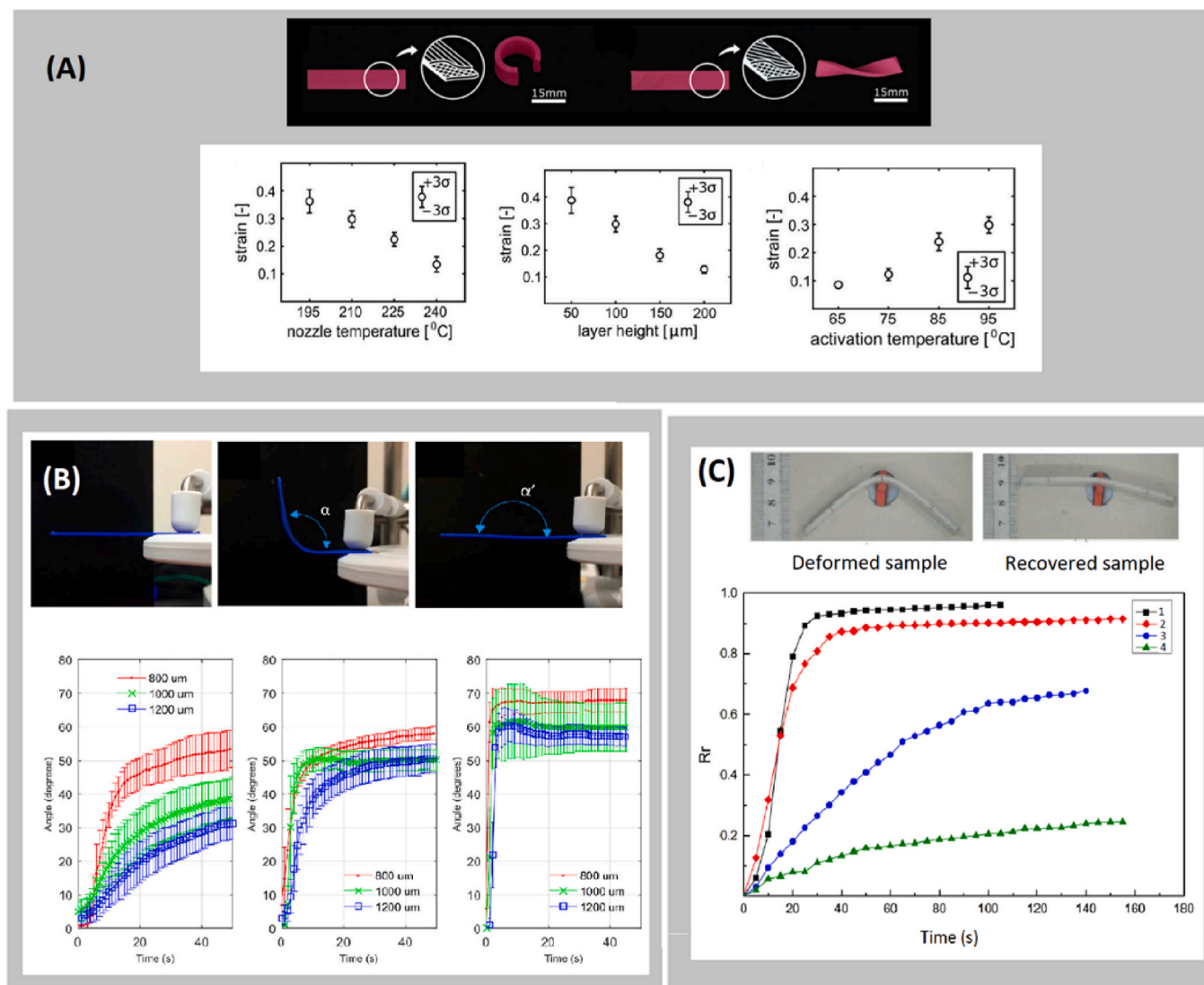
Fig. 15. (A) Shape transformations can be programmed during the printing process to fabricate either self-bending or self-twisting depending on the exact orientation of a top layer on a multi-ply print (top), Various parameters impact strain in the multi-ply panels including nozzle temperature, layer height, and activation temperature (bottom), reproduced from Ref. [153]; (B) Shape recovery process of a flat PLA sample: first, the flat printed sample is programmed at a 90° angle in the water at 70 °C, then cooled down to T_g to keep the new form. For the recovery process, the cantilever was submersed again in the bath and the bending angle (α') was recorded after 45–60 s intervals. (Bottom) Variation in the unbending angle for 800, 1000, and 1200 μm thick PLA cantilevers exposed to 65 °C, 75 °C, and 85 °C water. Reproduced from Ref. [122]; (C) Variation of the shape-recovery ratio Rr of PLA samples with time under varying conditions including (1) T_d = 55 °C, T_r = 70 °C, θ = 0°, H = 300 μm; (2) T_d = 55 °C, T_r = 65 °C, θ = 30°, H = 100 μm; (3) T_d = 55 °C, T_r = 60 °C, θ = 45°, H = 200 μm; and (4) T_d = 55 °C, T_r = 55 °C, θ = 15°, H = 150, θ = 15°, H = 150 μm, reproduced from Ref. [155].

with sufficient chain mobility to support prompt recovery to the original shape. At 70 °C, R_r exceeded 90 % within 30 s and reached a maximum value of 98 %. In contrast, for curves *c* and *d* where T_r is less than T_g, adequate chain mobility cannot be achieved and so only partial recovery at a lower rate is observed. For instance, at 55 °C, R_r did not reach 25 % after nearly 3 minutes [155].

Fig. 16(A) shows the design and programming process of a 3D printed origami structure reported by *Mehrpouya* et al. [129]. The planar structure consists of a square surrounded by four triangles, each of which shares an edge with the square. Through heating in a water bath, the folded structure can be reverted into its planar form, i.e. the programmed sample can restore its initial flat shape in almost 30 seconds. The right side of this figure illustrates a variation in recovery ratio in several independently considered printing parameters, including activation temperature, layer height, nozzle temperature, and total thickness. It shows that an increase in the activation temperature, layer height, and nozzle temperature can significantly enhance the shape

recovery ratio of the printed structures while the increase of the total thickness can have an opposite effect on the shape recovery process. Fig. 16(B) also represents the impact of recovery temperature on the shape recovery behavior of the deformed sample. As visible, the Miura-origami sheet is deformed to a flat 2D shape, and then the temperature stimulus iduces recovery of its initial S-shape. The plot of shape recovery vs. time shows that the deformed specimen can recover its initial shape significantly faster at a higher temperature (90 °C) compared to the other temperatures. However, using very hot water, over a temperature of 95 °C, can create permanent damage due to crystallization in the material during the heating process [108].

3.4. Advantages and challenges

By introducing temporal variation into the part specification and design, 4D printing enables a multitude of novel and unique applications. Despite its novelty, the fabrication process for 4D printing is
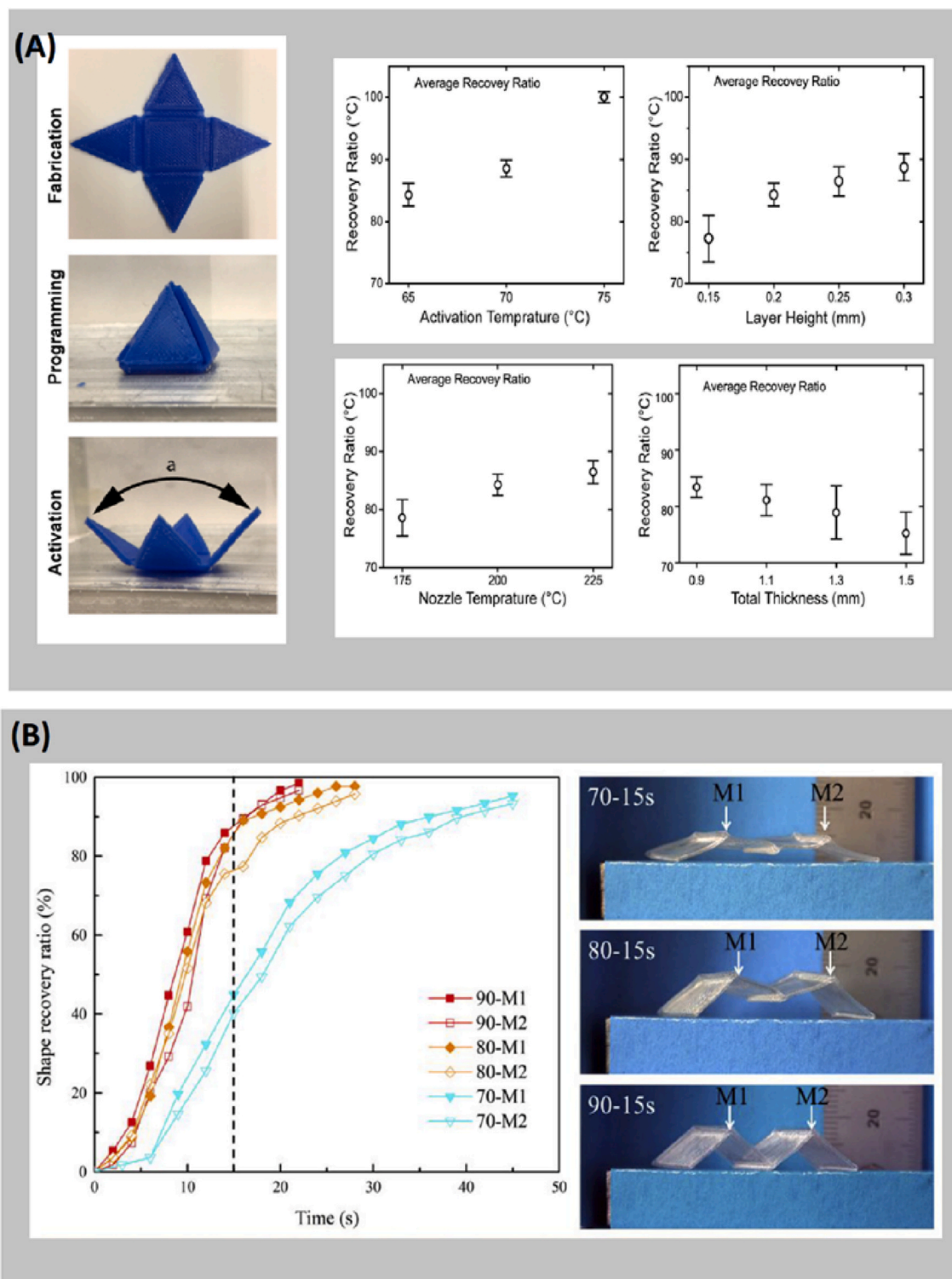
Fig. 16. The design and shape recovery process of the printed origami structures; (A) The fabrication, programming, and activation printed pyramid (left), The recovery ratio of the specimens for different activation temperatures, nozzle temperatures, layer heights, and total thickness (right), reproduced from Ref. [129], (B) Shape recovery behavior of printed Miura-Origami sheet versus time (in 15 s) at various recovery temperatures (70 °C, 80 °C, and 90 °C), reproduced from Ref. [130].

essentially identical to 3D printing. Temporal variation is enabled through the careful design of a 3D-printed part with a suitable choice of printing material [21,156]. As outlined in this review, even well-established 3D printing materials such as PLA can function as smart materials for supporting 4D printing projects using various printing methods, even inexpensive FDM printers. Nonetheless, expanding material options is a principal challenge for further expansion of 4D

printing. Beyond identifying a material that responds favorably to an external stimulus, certain applications will require materials that respond to specific stimuli. Augmenting the catalog of materials available for 4D printing – in terms of mechanical properties and associated stimulus – is a key direction for the future development of 4D printing [157]. Especially for *in vivo* biomedical applications, identifying materials that can preserve shape-memory properties over large numbers of
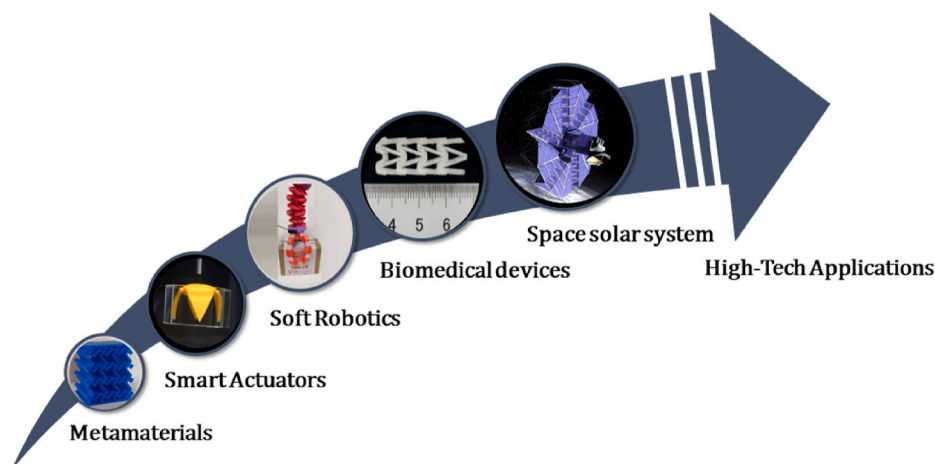
Fig. 17. The potential and future applications of the 4D printing technology of PLA biopolymer.

deformation cycles is critically important.

Additionally, further customization in change-inducing stimuli must be achieved to be able to remotely and precisely trigger and control shape changes. User-level challenges in 4D printing stem largely from the difficulty of designing a structure that will facilitate the desired transformation into a targeted shape. In practice, achieving elaborate transformations requires building supplementary components to support material programming, printing with multiple materials, and implementing innovative printing techniques and interfaces for achieving motions such as folding, curling, twisting, and linear expansion and shrinkage. The application of multiple SMPs can provide a great opportunity for designing more complex 3D motion, e.g. mechanical meta-structures, and control the temporal evolution of the 3D structure to match the geometrical complexity of the printed structure, such as 3D printed structures with different shape recovery behavior [134,158].

At the design phase, sophisticated calculations and modeling are required for simulating transformations given a specific design and associated material properties and constraints. Without adequate simulation tools, 4D printing can present a hopelessly complicated process for even simple tasks [159]. Even at present, deformations that have been demonstrated in 4D printing applications have been limited to simple transformations such as self-folding and bending. The future success of 4D printing will depend critically on the continued development of tools for precisely modeling responses of printed objects to external stimuli [160]. Besides, creativity in designs will help to develop a new generation of smart products with a diverse range of applications in various fields and industrial domains. Fig. 17 represents the potential and future applications of the 4D printing technology of PLA biopolymer.

4. Summary

4D printing has generated substantial excitement and attention since its recent introduction. Diverse applications have been demonstrated using various printing methods, materials, and actuation mechanisms. These applications have sparked interests in 4D printing in a variety of fields, notably including biomedical engineering. Developments achieved specifically with PLA – an inexpensive, biodegradable, and well-established polymer – highlight the promise for further development of 4D printing. Thanks to its excellent shape memory properties, biocompatibility, and easy processing, PLA will remain a compelling material for further development of 4D printing designs. Beyond PLA, exciting research continues to introduce materials and approaches such as composites that combine PLA with nanomaterials for achieving novel designs.

Declaration of competing interest

The authors declare that they have no known competing financial interests or personal relationships that could have appeared to influence the work reported in this paper.

References

[1] A. Savini, G. Savini, A short history of 3D printing, a technological revolution just started, in: ICOHTEC/IEEE International History of High-Technologies and Their Socio-Cultural Contexts Conference (HISTELCON). 2015, IEEE, 2015.

[2] Z.X. Khoo, et al., 3D printing of smart materials: a review on recent progresses in 4D printing, Virtual Phys. Prototyp. 10 (3) (2015) 103–122.

[3] C.L. Ventola, Medical applications for 3D printing: current and projected uses, Pharm. Therapeut. 39 (10) (2014) 704.

[4] D. Lin, et al., Three-dimensional printing of complex structures: man made or toward nature? ACS Nano 8 (10) (2014) 9710–9715.

[5] B. Berman, 3-D printing: the new industrial revolution, Bus. Horiz. 55 (2) (2012) 155–162.

[6] M. Mehrpouya, et al., The potential of additive manufacturing in the smart factory industrial 4.0: a review, Appl. Sci. 9 (18) (2019) 3865.

[7] M. Mehrpouya, et al., The benefits of additive manufacturing for sustainable design and production, in: Sustainable Manufacturing, Elsevier, 2021, pp. 29–59.

[8] S.H. Huang, et al., Additive manufacturing and its societal impact: a literature review, Int. J. Adv. Manuf. Technol. 67 (5–8) (2013) 1191–1203.

[9] W. Yang, et al., Advanced shape memory technology to reshape product design, manufacturing and recycling, Polymers 6 (8) (2014) 2287–2308.

[10] B.C. Gross, et al., Evaluation of 3D Printing and its Potential Impact on Biotechnology and the Chemical Sciences, ACS Publications, 2014.

[11] F. Krujatz, et al., Additive Biotech—chances, challenges, and recent applications of additive manufacturing technologies in biotechnology, New Biotechnol. 39 (2017) 222–231.

[12] A. Gisario, et al., Metal additive manufacturing in the commercial aviation industry: a review, J. Manuf. Syst. 53 (2019) 124–149.

[13] T.D. Ngo, et al., Additive manufacturing (3D printing): a review of materials, methods, applications and challenges, Compos. B Eng. 143 (2018) 172–196.

[14] H. Vahabi, et al., Flame retardant polymer materials: an update and the future for 3D printing developments, Mater. Sci. Eng. R Rep. 144 (2021) 100604.

[15] P. Zarrintaj, et al., Nanocomposite biomaterials made by 3D printing: achievements and challenges, in: Handbook of Polymer Nanocomposites for Industrial Applications, Elsevier, 2021, pp. 675–685.

[16] H. Ding, et al., Review of mechanisms and deformation behaviors in 4D printing, Int. J. Adv. Manuf. Technol. 105 (11) (2019) 4633–4649.

[17] S. Miao, et al., 4D printing of polymeric materials for tissue and organ regeneration, Mater. Today 20 (10) (2017) 577–591.

[18] A.S. Gladman, et al., Biomimetic 4D printing, Nat. Mater. 15 (4) (2016) 413–418.

[19] X. Kuang, et al., Advances in 4D printing: materials and applications, Adv. Funct. Mater. 29 (2) (2019) 1805290.

[20] A. Mitchell, et al., Additive manufacturing—a review of 4D printing and future applications, Addit. Manuf. 24 (2018) 606–626.

[21] H. Ding, et al., Review of mechanisms and deformation behaviors in 4D printing, Int. J. Adv. Manuf. Technol. (2019) 1–17.

[22] S.K. Leist, J. Zhou, Current status of 4D printing technology and the potential of light-reactive smart materials as 4D printable materials, Virtual Phys. Prototyp. 11 (4) (2016) 249–262.

[23] Q. Ge, et al., Multimaterial 4D printing with tailorable shape memory polymers, Sci. Rep. 6 (2016) 31110.

[24] J. Wu, et al., Multi-shape active composites by 3D printing of digital shape memory polymers, Sci. Rep. 6 (2016) 24224.

[25] S. Miao, et al., Four-dimensional printing hierarchy scaffolds with highly biocompatible smart polymers for tissue engineering applications, Tissue Eng. C Methods 22 (10) (2016) 952–963.

[26] C. Liu, H. Qin, P. Mather, Review of progress in shape-memory polymers, J. Mater. Chem. 17 (16) (2007) 1543–1558.

[27] H. Meng, G. Li, A review of stimuli-responsive shape memory polymer composites, Polymer 54 (9) (2013) 2199–2221.

[28] K.K. Patel, R. Purohit, Future prospects of shape memory polymer nano-composite and epoxy based shape memory polymer-a review, Mater. Today: Proc. 5 (9) (2018) 20193–20200.

[29] W.M. Huang, et al., Thermo/chemo-responsive shape memory effect in polymers: a sketch of working mechanisms, fundamentals and optimization, J. Polym. Res. 19 (9) (2012) 9952.

[30] M. Behl, M.Y. Razzaq, A. Lendlein, Multifunctional shape-memory polymers, Adv. Mater. 22 (31) (2010) 3388–3410.

[31] F.S. Senatov, et al., Mechanical properties and shape memory effect of 3D-printed PLA-based porous scaffolds, J. Mech. Behav. Biomed. Mater. 57 (2016) 139–148.

[32] I.A. Rousseau, Challenges of shape memory polymers: a review of the progress toward overcoming SMP's limitations, Polym. Eng. Sci. 48 (11) (2008) 2075–2089.

[33] F. Memarian, et al., Thermo-mechanical and shape memory behavior of TPU/ABS/MWCNTs nanocomposites compatibilized with ABS-g-MAH, Polym. Compos. 40 (2) (2019) 789–800.

[34] A.M. DiOrio, et al., A functionally graded shape memory polymer, Soft Matter 7 (1) (2011) 68–74.

[35] Q. Zhao, H.J. Qi, T. Xie, Recent progress in shape memory polymer: new behavior, enabling materials, and mechanistic understanding, Prog. Polym. Sci. 49 (2015) 79–120.

[36] L. Sun, et al., A brief review of the shape memory phenomena in polymers and their typical sensor applications, Polymers 11 (6) (2019) 1049.

[37] M. Radjabian, M. Kish, N. Mohammadi, Structure–property relationship for poly (lactic acid)(PLA) filaments: physical, thermomechanical and shape memory characterization, J. Polym. Res. 19 (9) (2012) 9870.

[38] W. Wang, et al., Polylactide-based polyurethane and its shape-memory behavior, Eur. Polym. J. 42 (6) (2006) 1240–1249.

[39] Q. Zhang, et al., Pattern transformation of heat-shrinkable polymer by three-dimensional (3D) printing technique, Sci. Rep. 5 (2015) 8936.

[40] M.H. Khaliq, et al., On the use of high viscosity polymers in the fused filament fabrication process, Rapid Prototyp. J. 23 (4) (2017).

[41] T. Fang, et al., Synthesis and study of shape-memory polymers selectively induced by near-infrared lights via in situ copolymerization, Polymers 9 (5) (2017) 181.

[42] M. Zarek, et al., 3D printing of shape memory polymers for flexible electronic devices, Adv. Mater. 28 (22) (2016) 4449–4454.

[43] X. Wu, et al., Mechanisms of the shape memory effect in polymeric materials, Polymers 5 (4) (2013) 1169–1202.

[44] L. Sun, et al., An overview of elastic polymeric shape memory materials for comfort fitting, Mater. Des. 136 (2017) 238–248.

[45] X. Luo, P.T. Mather, Preparation and characterization of shape memory elastomeric composites, Macromolecules 42 (19) (2009) 7251–7253.

[46] T. Takahashi, N. Hayashi, S. Hayashi, Structure and properties of shape-memory polyurethane block copolymers, J. Appl. Polym. Sci. 60 (7) (1996) 1061–1069.

[47] M.R. Saeb, et al., Unspoken aspects of chain shuttling reactions: patterning the molecular landscape of olefin multi-block copolymers, Polymer 116 (2017) 55–75.

[48] L. Sun, et al., Heating-responsive shape-memory effect in thermoplastic polyurethanes with low melt-flow index, Macromol. Chem. Phys. 215 (24) (2014) 2430–2436.

[49] J. Xu, J. Song, Thermal responsive shape memory polymers for biomedical applications, Biomed. Eng. Front. Chall (2011) 125–142.

[50] C.L. Lewis, E.M. Dell, A review of shape memory polymers bearing reversible binding groups, J. Polym. Sci. B Polym. Phys. 54 (14) (2016) 1340–1364.

[51] M.-Y. Shie, et al., Review of polymeric materials in 4D printing biomedical applications, Polymers 11 (11) (2019) 1864.

[52] H. Vahabi, et al., Inclusion of modified lignocellulose and nano-hydroxyapatite in development of new bio-based adjuvant flame retardant for poly (lactic acid), Thermochim. Acta 666 (2018) 51–59.

[53] E.R. Rad, et al., Bio-epoxy resins with inherent flame retardancy, Prog. Org. Coating 135 (2019) 608–612.

[54] H. Vahabi, et al., Biodegradable polyester thin films and coatings in the line of fire: the time of polyhydroxyalkanoate (PHA)? Prog. Org. Coating 133 (2019) 85–89.

[55] M. Mehrpouya, et al., Additive manufacturing of polyhydroxyalkanoates (PHAs) biopolymers: materials, printing techniques, and applications, Mater. Sci. Eng. C (2021) 112216.

[56] V. Nagarajan, A.K. Mohanty, M. Misra, Perspective on polylactic acid (PLA) based sustainable materials for durable applications: focus on toughness and heat resistance, ACS Sustain. Chem. Eng. 4 (6) (2016) 2899–2916.

[57] R.A. Auras, et al., Poly (Lactic Acid): Synthesis, Structures, Properties, Processing, and Applications, vol. 10, John Wiley & Sons, 2011.

[58] R.a. markets, Global polylactic acid (PLA) market for 3D printing, in: Printing Market Research Reports, 2019, p. 266.

[59] K.M. Nampoothiri, N.R. Nair, R.P. John, An overview of the recent developments in polylactide (PLA) research, Bioresour. Technol. 101 (22) (2010) 8493–8501.

[60] L. Xiao, et al., Poly (lactic acid)-based biomaterials: synthesis, modification and applications, Biomed. Sci. Eng. Technol. (2012) 11.

[61] S. Su, et al., Polylactide (PLA) and its blends with poly (butylene succinate)(PBS): a brief review, Polymers 11 (7) (2019) 1193.

[62] K. Masutani, Y. Kimura, PLA Synthesis. From the Monomer to the Polymer, 2014.

[63] M. Lopes, A. Jardini Filho, Synthesis and characterizations of poly (lactic acid) by ring-opening polymerization for biomedical applications, Chem. Eng. 38 (2014) 331–336.

[64] Y. Hu, et al., Newly developed techniques on polycondensation, ring-opening polymerization and polymer modification: focus on poly (lactic acid), Materials 9 (3) (2016) 133.

[65] N. Work, 3D series for 3D printing, 2020. Available from: https://www.natur eworksllc.com/Products/3D-series-for-3D-printing.

[66] S. Farah, D.G. Anderson, R. Langer, Physical and mechanical properties of PLA, and their functions in widespread applications—a comprehensive review, Adv. Drug Deliv. Rev. 107 (2016) 367–392.

[67] L.-T. Lim, R. Auras, M. Rubino, Processing technologies for poly (lactic acid), Prog. Polym. Sci. 33 (8) (2008) 820–852.

[68] S. Saeidlou, et al., Poly (lactic acid) crystallization, Prog. Polym. Sci. 37 (12) (2012) 1657–1677.

[69] M. Nofar, R. Salehiyan, S.S. Ray, Influence of nanoparticles and their selective localization on the structure and properties of polylactide-based blend nanocomposites, Compos. B Eng. (2021) 108845.

[70] X. Zhao, et al., Super tough poly (lactic acid) blends: a comprehensive review, RSC Adv. 10 (22) (2020) 13316–13368.

[71] M.D. Hager, et al., Shape memory polymers: past, present and future developments, Prog. Polym. Sci. 49–50 (2015) 3–33.

[72] G.J. Berg, et al., New directions in the chemistry of shape memory polymers, Polymer 55 (23) (2014) 5849–5872.

[73] J. Xu, J. Song, Polylactic Acid (PLA)-based Shape-Memory Materials for Biomedical Applications, Shape Memory Polymers for Biomedical Applications, 2015, pp. 197–217.

[74] W.M. Huang, et al., Instability/collapse of polymeric materials and their structures in stimulus-induced shape/surface morphology switching, Mater. Des. 59 (2014) 176–192.

[75] C. Renata, W.M. Huang, J.J. Yang, Shape change/memory actuators based on shape memory materials, J. Mech. Sci. Technol. 31 (10) (2017) 4863–4873.

[76] U. Meekum, A. Khiansanoi, PLA and two components silicon rubber blends aiming for frozen foods packaging applications, Results Phys. 8 (2018) 79–88.

[77] J. Muller, C. González-Martínez, A. Chiralt, Combination of poly (lactic) acid and starch for biodegradable food packaging, Materials 10 (8) (2017) 952.

[78] P. Claro, et al., Biodegradable blends with potential use in packaging: a comparison of PLA/chitosan and PLA/cellulose acetate films, J. Polym. Environ. 24 (4) (2016) 363–371.

[79] Y. Wang, M.A. Hillmyer, Polyethylene-poly (L-lactide) diblock copolymers: synthesis and compatibilization of poly (L-lactide)/polyethylene blends, J. Polym. Sci. Polym. Chem. 39 (16) (2001) 2755–2766.

[80] K.S. Anderson, M.A. Hillmyer, The influence of block copolymer microstructure on the toughness of compatibilized polylactide/polyethylene blends, Polymer 45 (26) (2004) 8809–8823.

[81] K.S. Anderson, S.H. Lim, M.A. Hillmyer, Toughening of polylactide by melt blending with linear low-density polyethylene, J. Appl. Polym. Sci. 89 (14) (2003) 3757–3768.

[82] R.G. Sinclair, Blends of Polyactic Acid, Google Patents, 1993.

[83] G. Biresaw, C. Carriere, Interfacial tension of poly (lactic acid)/polystyrene blends, J. Polym. Sci. B Polym. Phys. 40 (19) (2002) 2248–2258.

[84] L. Zhang, S. Goh, S. Lee, Miscibility and crystallization behaviour of poly (L-lactide)/poly (p-vinylphenol) blends, Polymer 39 (20) (1998) 4841–4847.

[85] C.-H. Ho, et al., Synthesis and characterization of TPO–PLA copolymer and its behavior as compatibilizer for PLA/TPO blends, Polymer 49 (18) (2008) 3902–3910.

[86] S. Ishida, et al., Toughening of poly (L-lactide) by melt blending with rubbers, J. Appl. Polym. Sci. 113 (1) (2009) 558–566.

[87] H.-J. Jin, et al., Blending of poly (L-lactic acid) with poly (cis-1, 4-isoprene), Eur. Polym. J. 36 (1) (2000) 165–169.

[88] X. Chen, et al., Chemical and morphological analysis of surface enrichment in a biodegradable polymer blend by phase-detection imaging atomic force microscopy, Macromolecules 31 (7) (1998) 2278–2283.

[89] M. Davies, et al., Surface analysis of biodegradable polymer blends of poly (sebacic anhydride) and poly (DL-lactic acid), Macromolecules 29 (6) (1996) 2205–2212.

[90] D. Newman, et al., Molecular mobilities in biodegradable poly (DL-lactic)/poly (ε-caprolactone) blends, Macromolecules 42 (14) (2009) 5219–5225.

[91] A. Bhatia, et al., Compatibility of biodegradable poly (lactic acid)(PLA) and poly (butylene succinate)(PBS) blends for packaging application, Korea Aust. Rheol. J. 19 (3) (2007) 125–131.

[92] N. Zhang, et al., Preparation and properties of biodegradable poly (lactic acid)/poly (butylene adipate-co-terephthalate) blend with glycidyl methacrylate as reactive processing agent, J. Mater. Sci. 44 (1) (2009) 250–256.

[93] F. Signori, M.-B. Coltelli, S. Bronco, Thermal degradation of poly (lactic acid) (PLA) and poly (butylene adipate-co-terephthalate)(PBAT) and their blends upon melt processing, Polym. Degrad. Stabil. 94 (1) (2009) 74–82.

[94] Y. Li, H. Shimizu, Toughening of polylactide by melt blending with a biodegradable poly (ether) urethane elastomer, Macromol. Biosci. 7 (7) (2007) 921–928.

[95] J.E. Mark, Some novel polymeric nanocomposites, Acc. Chem. Res. 39 (12) (2006) 881–888.

[96] H.W. Kim, H.H. Lee, J. Knowles, Electrospinning biomedical nanocomposite fibers of hydroxyapatite/poly (lactic acid) for bone regeneration, J. Biomed. Mater. Res. Part A 79 (3) (2006) 643–649. An Official Journal of The Society for Biomaterials, The Japanese Society for Biomaterials, and The Australian Society for Biomaterials and the Korean Society for Biomaterials.

[97] R. Hiroi, et al., Organically modified layered titanate: a new nanofiller to improve the performance of biodegradable polylactide, Macromol. Rapid Commun. 25 (15) (2004) 1359–1364.

[98] E. Fortunati, et al., Multifunctional bionanocomposite films of poly (lactic acid), cellulose nanocrystals and silver nanoparticles, Carbohydr. Polym. 87 (2) (2012) 1596–1605.

[99] E. Fortunati, et al., Microstructure and nonisothermal cold crystallization of PLA composites based on silver nanoparticles and nanocrystalline cellulose, Polym. Degrad. Stabil. 97 (10) (2012) 2027–2036.

[100] K. Fukushima, et al., Effect of expanded graphite/layered-silicate clay on thermal, mechanical and fire retardant properties of poly (lactic acid), Polym. Degrad. Stabil. 95 (6) (2010) 1063–1076.

[101] M.R. Aghjeh, et al., Depth analysis of micro-mechanism of mechanical property alternations in PLA/EVA/clay nanocomposites: a combined theoretical and experimental approach, Mater. Des. 88 (2015) 1277–1289.

[102] M. Iturrondobeitia, et al., Semi-automated quantification of the microstructure of PLA/clay nanocomposites to improve the prediction of the elastic modulus, Polym. Test. 66 (2018) 280–291.

[103] F. Momeni, X. Liu, J. Ni, A review of 4D printing, Mater. Des. 122 (2017) 42–79.

[104] M. Bodaghi, et al., 4D printing self-morphing structures, Materials 12 (8) (2019) 1353.

[105] A. Le Duigou, et al., A Review of 3D and 4D Printing of Natural Fibre Biocomposites, Materials & Design, 2020, p. 108911.

[106] E. Pei, G.H. Loh, Technological considerations for 4D printing: an overview, Prog. Addit. Manuf. 3 (1–2) (2018) 95–107.

[107] M. Monzón, et al., 4D printing: processability and measurement of recovery force in shape memory polymers, Int. J. Adv. Manuf. Technol. 89 (5–8) (2017) 1827–1836.

[108] Y. Zhou, et al., From 3D to 4D printing: approaches and typical applications, J. Mech. Sci. Technol. 29 (10) (2015) 4281–4288.

[109] S.E. Bakarich, et al., 4D printing with mechanically robust, thermally actuating hydrogels, Macromol. Rapid Commun. 36 (12) (2015) 1211–1217.

[110] C.M. González-Henríquez, M.A. Sarabia-Vallejos, J. Rodriguez-Hernandez, Polymers for additive manufacturing and 4D-printing: materials, methodologies, and biomedical applications, Prog. Polym. Sci. 94 (2019) 57–116.

[111] A.A. D`Amico, A. Debaie, A.M. Peterson, Effect of layer thickness on irreversible thermal expansion and interlayer strength in fused deposition modeling, Rapid Prototyp. J. 23 (5) (2017) 943–953.

[112] F. Hu, et al., Origami spring–inspired metamaterials and robots: an attempt at fully programmable robotics, Sci. Prog. 103 (3) (2020), 0036850420946162.

[113] P.S. Poh, et al., Polylactides in additive biomanufacturing, Adv. Drug Deliv. Rev. 107 (2016) 228–246.

[114] J.K. Oh, Polylactide (PLA)-based amphiphilic block copolymers: synthesis, self-assembly, and biomedical applications, Soft Matter 7 (11) (2011) 5096–5108.

[115] B. Tyler, et al., Polylactic acid (PLA) controlled delivery carriers for biomedical applications, Adv. Drug Deliv. Rev. 107 (2016) 163–175.

[116] A.J. Lasprilla, et al., Poly-lactic acid synthesis for application in biomedical devices—a review, Biotechnol. Adv. 30 (1) (2012) 321–328.

[117] D.G. Tamay, et al., 3D and 4D printing of polymers for tissue engineering applications, Front. Bioeng. Biotechnol. 7 (2019).

[118] B. An, et al., Thermorph: democratizing 4D printing of self-folding materials and interfaces, in: Proceedings of the 2018 CHI Conference on Human Factors in Computing Systems, 2018.

[119] M. Carlson, Y. Li, Development and kinetic evaluation of a low-cost temperature-sensitive shape memory polymer for 4-dimensional printing, Int. J. Adv. Manuf. Technol. 106 (9) (2020) 4263–4279.

[120] S. Zhang, et al., Shape memory Poly (lactic acid) binary blends with unusual fluorescence, Polymer 209 (2020) 122980.

[121] M.M. Hanon, L. Zsidai, Q. Ma, Accuracy investigation of 3D printed PLA with various process parameters and different colors, Mater. Today: Proc. 42 (2021) 3089–3096.

[122] S.K. Leist, et al., Investigating the shape memory properties of 4D printed polylactic acid (PLA) and the concept of 4D printing onto nylon fabrics for the creation of smart textiles, Virtual Phys. Prototyp. 12 (4) (2017) 290–300.

[123] Y. Wang, X. Li, An accurate finite element approach for programming 4D-printed self-morphing structures produced by fused deposition modeling, Mech. Mater. 151 (2020) 103628.

[124] A.P. Valerga, et al., Influence of PLA filament conditions on characteristics of FDM parts, Materials 11 (8) (2018) 1322.

[125] C.-Y. Chang, Study on the correlation between humidity and material strains in separable micro humidity sensor design, Sensors 17 (5) (2017) 1066.

[126] L. Fang, et al., Effects of environmental temperature and humidity on the geometry and strength of polycarbonate specimens prepared by fused filament fabrication, Materials 13 (19) (2020) 4414.

[127] Q. Zhang, K. Zhang, G. Hu, Smart three-dimensional lightweight structure triggered from a thin composite sheet via 3D printing technique, Sci. Rep. 6 (2016) 22431.

[128] H. Liu, H. He, B. Huang, Favorable thermoresponsive shape memory effects of 3D printed poly (lactic acid)/poly (ε-Caprolactone) blends fabricated by fused deposition modeling, Macromol. Mater. Eng. 305 (11) (2020) 2000295.

[129] M. Mehrpouya, et al., Investigation on the functionality of thermo-responsive origami structures, Adv. Eng. Mater. 22 (8) (2020).

[130] Y. Liu, et al., Shape memory behavior and recovery force of 4D printed laminated Miura-origami structures subjected to compressive loading, Compos. B Eng. 153 (2018) 233–242.

[131] X. Xin, et al., Origami-inspired self-deployment 4D printed honeycomb sandwich structure with large shape transformation, Smart Mater. Struct. 29 (6) (2020), 065015.

[132] X. Xin, et al., 4D printing auxetic metamaterials with tunable, programmable, and reconfigurable mechanical properties, Adv. Funct. Mater. 30 (43) (2020) 2004226.

[133] R. Noroozi, et al., Shape-adaptive metastructures with variable bandgap regions by 4D printing, Polymers 12 (3) (2020) 519.

[134] M. Mirzaali, et al., Multi-material 3D printed mechanical metamaterials: rational design of elastic properties through spatial distribution of hard and soft phases, Appl. Phys. Lett. 113 (24) (2018) 241903.

[135] S. Singh, et al., 3D printed biodegradable composites: an insight into mechanical properties of PLA/chitosan scaffold, Polym. Test. 89 (2020) 106722.

[136] N. Poomathi, et al., 3D printing in tissue engineering: a state of the art review of technologies and biomaterials, Rapid Prototyp. J. 26 (7) (2020).

[137] M. Barletta, A. Gisario, M. Mehrpouya, 4D printing of shape memory polylactic acid (PLA) components: investigating the role of the operational parameters in fused deposition modelling (FDM), J. Manuf. Process. 61 (2021) 473–480.

[138] M. Mehrpouya, et al., Investigation on shape recovery of 3D printed honeycomb sandwich structure, Polym. Adv. Technol. 31 (12) (2020) 3361–3365.

[139] H.Y. Sarvestani, et al., 3D printed architected polymeric sandwich panels: energy absorption and structural performance, Compos. Struct. 200 (2018) 886–909.

[140] T. Liu, et al., 4D printed anisotropic structures with tailored mechanical behaviors and shape memory effects, Compos. Sci. Technol. 186 (2020) 107935.

[141] Z. Wu, et al., Radial compressive property and the proof-of-concept study for realizing self-expansion of 3D printing polylactic acid vascular stents with negative Poisson's ratio structure, Materials 11 (8) (2018) 1357.

[142] W. Zhou, et al., 4D-Printed dynamic materials in biomedical applications: chemistry, challenges, and their future perspectives in the clinical sector, J. Med. Chem. 63 (15) (2020).

[143] G. Singh, et al., Characterization of three-dimensional printed thermal-stimulus polylactic acid-hydroxyapatite-based shape memory scaffolds, Polym. Compos. 41 (9) (2020) 3871–3891.

[144] A. Pandey, et al., 3D printed biodegradable functional temperature-stimuli shape memory polymer for customized scaffoldings, J. Mech. Behav. Biomed. Mater. (2020) 103781.

[145] C.-Y. Cheng, et al., 4D printing of shape memory aliphatic copolyester via UV-assisted FDM strategy for medical protective devices, Chem. Eng. J. (2020) 125242.

[146] M. Touri, et al., Additive manufacturing of biomaterials– the evolution of rapid prototyping, Adv. Eng. Mater. 21 (2) (2019) 1800511.

[147] S. Bodkhe, P. Ermanni, 3D printing of multifunctional materials for sensing and actuation: merging piezoelectricity with shape memory, Eur. Polym. J. (2020) 109738.

[148] H. Wei, et al., Direct-write fabrication of 4D active shape-changing structures based on a shape memory polymer and its nanocomposite, ACS Appl. Mater. Interfaces 9 (1) (2017) 876–883.

[149] Y. Dong, et al., 4D Printed Hydrogels: Fabrication, Materials, and Applications, Advanced Materials Technologies, 2020, p. 2000034.

[150] W. Zhao, et al., Personalized 4D printing of bioinspired tracheal scaffold concept based on magnetic stimulated shape memory composites, Compos. Sci. Technol. 184 (2019) 107866.

[151] A.M. Kelly, et al., Analysis of Shape Memory Properties in 3D Printed PLA, 2018.

[152] C. Barrett, J.K. Presing, One-Way 3D Printed Shape Memory Polymers, Worcester Polytechnic Institute, 2017.

[153] T. van Manen, S. Janbaz, A.A. Zadpoor, Programming 2D/3D shape-shifting with hobbyist 3D printers, Mater. Horiz. 4 (6) (2017) 1064–1069.

[154] S. Shin, H. So, Effect of 3D printing raster angle on reversible thermo-responsive composites using PLA/paper bilayer, Smart Mater. Struct. 29 (10) (2020) 105016.

[155] W. Wu, et al., Influence of layer thickness, raster angle, deformation temperature and recovery temperature on the shape-memory effect of 3D-printed polylactic acid samples, Materials 10 (8) (2017) 970.

[156] J. Choi, et al., 4D printing technology: a review, 3D Print. Addit. Manuf. 2 (4) (2015) 159–167.

[157] Y.S. Lui, et al., 4D printing and stimuli-responsive materials in biomedical aspects, Acta Biomater. 92 (2019) 19–36.

[158] M. Bodaghi, et al., Reversible energy absorbing meta-sandwiches by FDM 4D printing, Int. J. Mech. Sci. 173 (2020) 105451.

[159] S. Tibbits, et al., 4D Printing and Universal Transformation, 2014.

[160] B. Gao, et al., 4D bioprinting for biomedical applications, Trends Biotechnol. 34 (9) (2016) 746–756.

Mehrshad Mehrpouya earned his Ph.D. degree through a fellowship program from Sapienza University of Rome (Italy) in 2017. He is currently an Assistant Professor in the Department of Design, Production, and Management (DPM) at the University of Twente (UT). His research interests are directed toward Advanced Manufacturing, 3D/4D Printing, Functional Materials, and modeling.

Arash Darafsheh is an Associate Professor of Radiation Oncology, a certidied medical physicist by the American Board of Radiology (ABR), and the PI of the Optical Imaging and Dosimetry Lab at the Washington University School of Medicine. He earned a Ph.D. in optical science and engineering in 2013 from the University of North Carolina at Charlotte. His current research interets include optical methods in medical physics, novel radiation dosimeters, ultra-high dose rate radiation therapy, and super-resolution microscopy.

Henri Vahabi received his Ph.D. in Materials Science from the University of Montpellier, France, in 2011. Since then, he joined the University of Lorraine, France as an Associate Professor. His main research interests include flame retardancy of polymeric materials and nanocomposites. He has authored over 100 peer-reviewed scientific articles/book chapters.

Thomas Mazur is an Assistant Professor of Radiation Oncology at the Washington University School of Medicine. He joined the faculty in 2016. He received his Ph.D. in physics at The University of Texas at Austin in 2014. He is interested in the application and development of advanced technologies for improving radiation therapy.

Shahram Janbaz received his Ph.D. from TU Delft, the Netherlands. He is currently a Post-Doctoral researcher in the institute of physics at the University of Amsterdam. His research interests are mechanical and smart metamaterials.

Seeram Ramakrishna is the Director of the Center for Nanofibres and Nanotechnology at the National University of Singapore (NUS), which is ranked among the top 20 universities in the world. He is regarded as the modern father of electrospinning. He is an elected Fellow of UK Royal Academy of Engineering (FREng); Singapore Academy of Engineering; Indian National Academy of Engineering; and ASEAN Academy of Engineering & Technology. He is an elected Fellow of the International Union of Societies of Biomaterials Science and Engineering (FBSE); Institution of Engineers Singapore; ISTE, India; Institution of Mechanical Engineers and Institute of Materials, Minerals & Mining, UK; and American Association of the Advancement of Science; ASM International; American Society for Mechanical Engineers; American Institute for Medical & Biological Engineering, USA. He is an editor of Elsevier journal Current Opinion in Biomedical Engineering.